A Study of Crystallization in Bisphenol A Polycarbonate

Robin Farmer

Dissertation Submitted to the Faculty of the
Virginia Polytechnic Institute and State University
in partial fulfillment of the requirements for the degree of

MASTER OF SCIENCE
in
Materials Science and Engineering

Dr. Herve Marand, Chairman
Dr. Sean Corcoran
Dr. William Reynolds

November 16, 2001
Blacksburg, Virginia

Keywords: Bisphenol-A Polycarbonate, Induction Period, Isothermal Lamellar thickening

A Study of the Crystallization of Bisphenol-A Polycarbonate

Robin Farmer

(ABSTRACT)

The crystallization behavior of bisphenol-A polycarbonate (BAPC) was studied, focusing on the initial stage of crystallization and the secondary stage of crystallization. Bisphenol-A polycarbonate was the polymer chosen for this study because of its slow crystallization rate. With slow crystallization kinetics, the polymer morphology does not change when quenched below its glass transition temperature, enabling the study of different stages of crystallization through the frozen morphology.

The study of the initial stages of crystallization pertained to crystallization times prior to the growth of detectable crystallinity. This study employed BAPC because of the long induction period, a direct result of the slow crystallization kinetics. During the induction period of polycarbonate crystallized at 190°C there was no evidence of polymer chain ordering that was seen in literature for other polymers. The length of the induction period determined by differential scanning calorimetry and wide-angle X-ray diffraction varied by over 6 hours because differential scanning calorimetry can detect a smaller amount of crystallinity than wide-angle X-ray diffraction. Signs of pre-ordering in the literature could be a result of experimental sensitivity.

The study of the secondary crystallization dealt with the isothermal lamellar thickening of BAPC crystals during annealing, after crystallization for an extended period of time. Small-angle X-ray scattering and differential scanning calorimetry experiments were performed on bisphenol-A polycarbonate samples crystallized near 190°C for 8 days and annealed at either 223°C or 228°C for various times. The Gibbs-Thomson

relationship, which can be defined using the experiments mentioned, yielded two thermodynamic constants, the equilibrium melting temperature and the surface free energy. Including data from literature in the determination of the constants, the equilibrium melting temperature and surface free energy of BAPC is 303°C and 36.6mJ/m^2, respectively. Comparing the lamellar thickness measurements by small-angle X-ray diffraction with direct measurements by microscopy was difficult because the morphology of the polymer was not easily seen in the bulk using atomic force microscopy or scanning electron microscopy. Etching the sample was the most promising technique for future investigations of revealing the bulk morphology for direct lamellar thickness measurements. Crystallizing thin films of polycarbonate on calcite substrates allowed the measurement of lamellar thickness using scanning electron microscopy because the lamellae grow epitaxially to the substrate. The measurement of the long spacing in thin film samples was comparable to that of bulk samples.

Acknowledgments

I would like to thank Dr. Herve Marand for his guidance and support through the duration of this project. He was always willing to answer my every question, no matter how trivial. I also would like to thank my committee members, Dr. Sean Corcoran and Dr. William Reynolds, helping me through this project.

I am sincerely thankful to Dr. Azar Alizadeh for her help in learning techniques, understanding theory, and the guidance she gave during the tough times. Stephen McCartney and Dr. Eva Marand also deserve thanks for allowing the use of SEM, AFM and IR.

I would above all like to thank my family for always believing in me and teaching me that any goal I set forth is attainable. Their support and love helped me through this degree and I can never thank them enough.

Table of Contents

Table Of Figures

Table Of Tables

Chapter 1. Introduction

It is well known, for any material, that the physical properties can be directly correlated to the structure of the material. The morphology of a semicrystalline polymer is a direct consequence of polymer crystallization, and the morphology has a large effect on the polymer properties including melting point, modulus, and ductility. Polymer crystallization has been studied for the past fifty years because use of semicrystalline polymers in industrial applications has increased. Crystallization is a kinetic process for all materials, but the crystallization of polymers is more complex than that of other materials such as metals. Polymer crystallization occurs in three steps, identified as the initial or induction stage of crystallization, primary crystallization, and secondary crystallization. Numerous researchers have studied these three steps in crystallization for a number of different polymers. In this project, the crystallization of polycarbonate will be studied because of its extremely slow crystallization kinetics. Slow crystallization allows the polymer structure to be "frozen" at various stages of crystallization by quenching to room temperature (below the polymer's glass transition temperature), making a thorough investigation of all crystallization steps possible.

1.1 Initial Stages of Crystallization

The process of crystallization begins with nucleation of a crystalline phase from an amorphous, or melt, phase. Nucleation is a kinetic process in which sections of polymer chains adopt a unique and favorable conformation and a dense crystallographic packing to create a nucleus that will be the first building block for larger polymer crystals. The rate of nucleation is dependent upon the magnitude of the undercooling, i.e.

the difference between the equilibrium melting temperature and the crystallization temperature.

Three mechanisms have been proposed for the initial transformation of a liquid phase into a crystal phase: heterogeneous nucleation, homogeneous nucleation, and spinodal decomposition.

1.1.1 Homogeneous Nucleation

Homogeneous nucleation is usually described by the classical nucleation theory[1]. In the classical nucleation theory, an embryo, formed by parallel alignment of sections of polymer chains in identical conformations, grows and shrinks in size with the addition or removal of sections of polymer chains. As these are added to an embryo, the free energy increases until the embryo reaches a critical size, at which point the free energy of the system decreases with further addition, and the growth of the nucleus becomes a spontaneous process. Figure 1 shows the variation of free energy with nucleus size, ν. Although the plot is depicted by a straight line, the addition of polymer chains to a nucleus causes an oscillatory behavior in the free energy with size, as shown in the insert of Figure 1. This oscillatory behavior is associated with the initial adsorption of a section of a polymer chain onto the nucleus (increase in surface area and overall surface free energy), and its subsequent inclusion in the ordered structure (decrease in overall bulk free energy of the crystal). If, for simplicity, we assume a spherical shape for embryos and nuclei, the free energy of an embryo of radius R is given in Equation 1.

$$\Delta G = \frac{4\pi R^3}{3}\Delta G_C + 4\pi R^2\sigma \qquad \textbf{(1)}$$

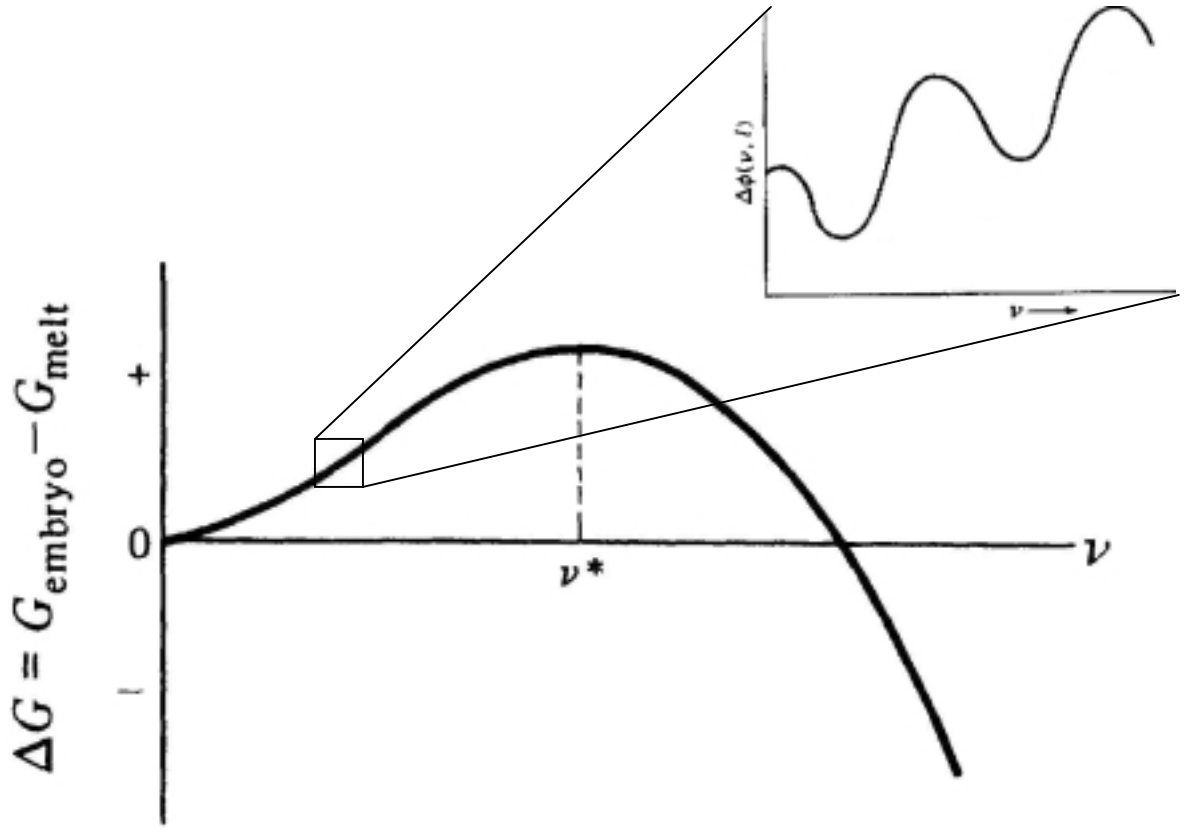

Figure 1. The Variation of Free Energy with Nucleus Size During Nucleation and Growth [1]

where ΔG_C is the bulk free energy of crystallization and σ is the crystal/melt interfacial free energy. The bulk free energy of crystallization can be expressed in terms of the latent heat of fusion and the undercooling ($T_m - T_x$) by:

$$\Delta G_C = \frac{-\Delta H_m \left(T_m - T_x\right)}{T_m} \quad \textbf{(2)}$$

The bulk free energy of crystallization is negative for crystallization temperatures, T_x, below the equilibrium melting temperature and positive above. For small radii, the free energy of formation of an embryo is dominated by interfacial effects and is positive. For large radii, the free energy of formation is negative as it is dominated by the bulk free energy of crystallization term. The critical embryo is defined by the radius R*, for which the free energy of formation is maximum. R* is therefore obtained by equating the derivative of the free energy of formation of an embryo with respect to embryo radius to zero. A simple mathematical derivation leads Equation 3

$$R^* = \frac{2T_m\sigma}{\Delta H_m \left(T_m - T_x\right)} \quad \textbf{(3)}$$

The free energy of formation of the critical nucleus is therefore given by:

$$\Delta G^* = \frac{16\pi T_m^2 \sigma^3}{3\Delta H_m^2 \left(T_m - T_x\right)^2} \quad \textbf{(4)}$$

Nucleation is therefore described in molecular terms as the transformation of a liquid phase to a crystal phase requiring passage over a free energy barrier of magnitude ΔG^*. The homogeneous nucleation rate is then given Equation 5

$$I = \frac{kT_x}{h} J\left(T_x\right) \exp\left(\frac{-\Delta G^*}{RT_x}\right) \quad \textbf{(5)}$$

where k is the Boltzmann's constant, h the Planck's constant and $J(T_x)$ a temperature dependent term that accounts for the mobility of polymer segments at the liquid-crystal interface (a term which depends on the difference between crystallization and glass transition temperatures).

Examination of the above equation suggests that the variation of the rate of homogeneous nucleation with crystallization temperature has a bell shaped curve with a maximum at temperatures between the glass transition and equilibrium melting temperatures. The nucleation rate approaches zero when the crystallization temperature approaches either the glass transition temperature or the equilibrium melting temperature. On the basis of this simple theory, one can also conclude that the dimensions of the critical nucleus decrease as the undercooling is increased. This latter observation results from the decrease in the barrier free energy of activation with increasing undercooling.

1.1.2 Heterogeneous Nucleation

Heterogeneous nucleation is the most common nucleation process in most materials. During heterogeneous nucleation, the formation of a crystalline nucleus occurs at the surface of an impurity present in the polymer melt (container wall, residual catalyst or simply dirt).[2] As in the case of homogeneous nucleation, the nucleus is composed of densely packed sections of polymer chains in a favorable conformation. However, in this case the nucleus stability is enhanced as a result of favorable interactions between the nucleus and the impurity surfaces. This enhanced stability leads to a decrease in the critical free energy barrier for nucleation at a given undercooling, thus to an increased nucleation rate.

1.1.3 Spinodal Decomposition

A third mechanism, namely, spinodal decomposition has been proposed to account for the initial transformation between liquid and crystal phases. It has been specifically proposed that spinodal decomposition could be a preordering process, which initiates the nucleation of a crystal phase from the melt. Spinodal decomposition can be viewed as the spatial separation of polymer chains into domains where chains have more conformational order and domains where the polymers chains have similar conformational order as in the usual melt. In this context, the spinodal decomposition process is characterized by spontaneous fluctuations identical in nature to those expected during the nematic ordering of a liquid crystalline material initially in the isotropic state. As the temperature is lowered, some favorable helical conformation become favorable in the melt state. These helical sections of polymer chains will be further stabilized if they can locally pack in a parallel arrangement. As this decomposition proceeds, regions of high (but non-crystalline) order develop and grow up to the point where the classical (see above) nucleation process can take place. It should be noted that the spinodal decomposition is a controversial model for the origin of the formation of nuclei. This mode has not been met with great enthusiasm in the polymer physics community.

1.2 Primary Crystallization

Primary crystallization is described as the stage subsequent to nucleation characterized by radial growth of crystalline lamellar structures from a central nucleus. Under isothermal conditions, lamellae grow at a constant rate at the expense of the melt by a chain folding mechanism. As the chain axis is usually perpendicular to the basal plane of the polymer lamellae, the lamellar thickness is also the distance between fold

planes parallel to the polymer chain axis. The thickness, which is controlled by the undercooling, is invariably much smaller than either the length or width of the lamellae. The surface free energy associated with the lateral sides of the lamellae is much lower than that of the folded surface, as the latter involves the work of chain folding (see Figure 2). While extended chain crystals are favored thermodynamically over chain folded crystals, the former would form at an infinitely slow rate and are not observed experimentally. At all crystallization temperatures, the observed morphology is lamellar and the observed thickness is the thickness of lamellae that grow the fastest. Lamellar growth is invariably accompanied by lamellar branching and splaying so much so that at some stage of the primary crystallization, the growing semicrystalline superstructure achieves spherical symmetry, and is therefore appropriately called a spherulite (Figure 3). Each spherulite is initiated by a single nucleus and grows until impingement with other spherulites, which defines the end of primary crystallization. Under isothermal condition, the variation of the degree of crystallinity with time exhibits a sigmoidal shape during primary crystallization. Previous studies of primary crystallization have clearly established that the crystallinity keeps increasing after spherulitic impingement. This further crystallization, termed secondary crystallization, is discussed in the next section.

1.3 Secondary Crystallization

Numerous researchers have studied secondary crystallization. Four main models have been developed to account for this increase in crystallinity after impingement. According to the lamellar insertion model, the increase in crystallinity is attributed to the growth of new lamellae between the lamellae formed during the primary crystallization.[4] In the lamellar thickening model, the increase in crystallinity is associated with the

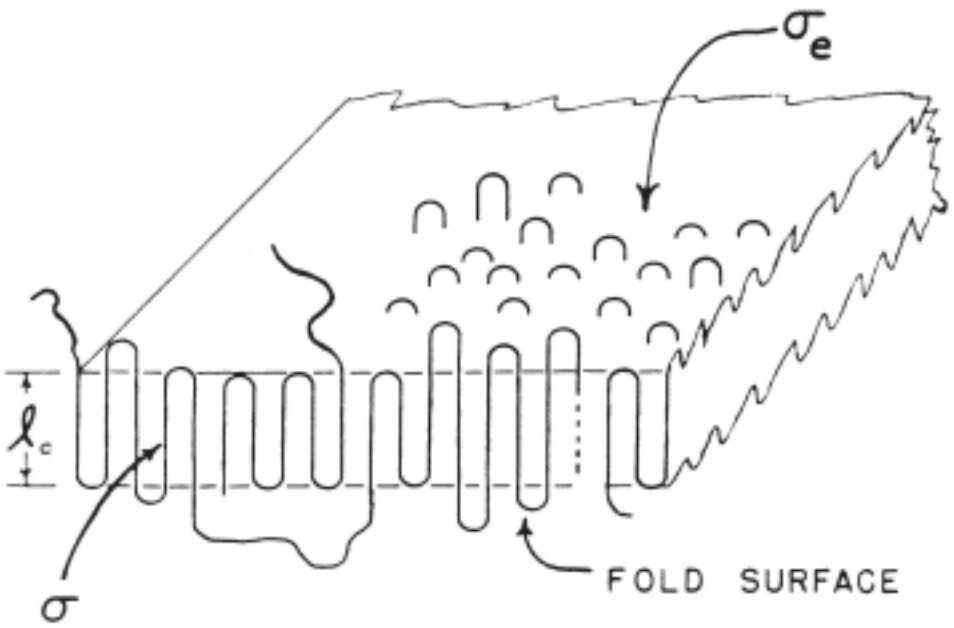

Figure 2. Single Crystal Lamellar Structure of a Polymer[3]

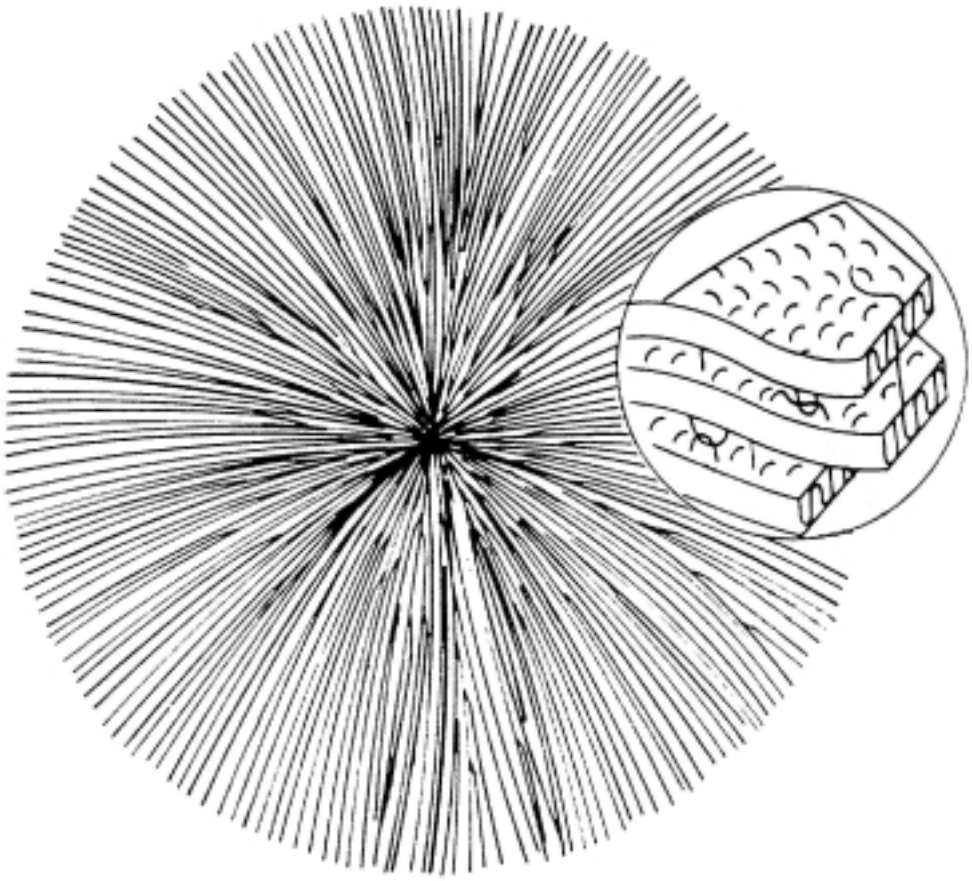

Figure 3. Schematic of a Polymer Spherulite with Radial Growth of Lamellae[3]

increase in lamellar thickness with time subsequent to their formation. The driving force for lamellar thickening is the decrease in the surface to volume ratio of thin polymer crystals.[5,6] In the crystal perfection model, the increase in crystallinity is associated with an increase in the degree of perfection of the crystals. This process involves the diffusion of defects out of the crystalline lamellae. Finally, in the fourth model, it is proposed that fringed-micellar crystals or mosaic block crystals form between primary lamellae.[6,7] While similar in spirit to the insertion model, this model predicts that, except at the highest temperatures, secondary crystals do not form by the chain folding mechanism, but rather by a local bundling of chain sequences into ordered structures of reduced lateral dimensions. While these four models of secondary crystallization have been debated within the polymer physics community during the last fifty years, some recent developments indicate that different mechanisms must be at play at low and high crystallization temperatures, respectively.

1.4 Project Scope

In recent years, attention has shifted from studies of primary or secondary crystallization to studies of the initial stage of crystallization (i.e. the induction period). Nucleation is a rare event that involves an infinitesimal fraction of a material's bulk and is believed to occur over a short time span. It is therefore not surprising that only few experiments have been designed to study directly the phenomenon of primary nucleation. Much of what we speculate about primary nucleation is based on the Classical Nucleation Theory, which was established to account for the temperature dependence of homogeneous nucleation rates. While this theory can be judged to be very successful, one should note that a quantitative fit of experimental data requires the use of adjustable

parameters, which cannot be measured independently. Furthermore, the use of macroscopic interfacial free energies to describe the energetics of systems often containing only few molecules or sections of chains has led to some skepticism. Recently, a number of proposals have appeared suggesting that nucleation of a crystal phase from a pure one-component melt might be preceded by an partial ordering process in the melt state which follows a spinodal decomposition kinetics.[4-8] The main reason for focusing on the initial stage of crystallization is related to the anticipated importance of melt structure and viscoelasticity on the processing, solidification and resulting properties of polymer products. To gain a better understanding of phenomena occurring during the induction period (time span before any significant level of crystallinity has developed) researchers have used polymers exhibiting a wide range of industrial applications. In the first section of this thesis, the initial stage of crystallization of bisphenol A polycarbonate will be studied. Even for crystallization under optimal conditions that maximize the rate of development of crystallinity, the induction period of polycarbonate is on the order of hours, allowing detailed study of the induction stage.

Although polymer chains go through three stages of crystallization, they never achieve full (100%) crystallinity. Two structures are present within a polymer specimen, the crystalline lamellae and an amorphous phase. As discussed earlier, polymer crystals must form by a chain folding mechanism because the equilibrium structure takes an infinite amount of time to form. In an ideal chain folded single crystal, such as grown from a dilute solution, one lamella would form with chains exiting and re-entering the crystal in adjacent positions. In reality when crystallization takes place from the melt state, lamellar formation is not perfect. Reentry can occur at any point along the lamella

face and chains can exit one lamella and enter into a neighboring lamella. The sections of chains that are kept out of the crystalline regions as a result of imperfect chain folding during lamellar growth may only crystallize with extreme difficulty during the secondary crystallization stage. The interlamellar region, therefore, remains primarily amorphous in nature. The morphology of a crystallizable polymer is therefore made up of these two phases, crystalline and amorphous, alternating throughout the polymer sample.

The most widely used instrumental tool for quantitative evaluation of submicron morphological features of semicrystalline polymers is small-angle x-ray scattering (SAXS). As a semicrystalline polymer is placed in the path of a monochromatic beam of x-rays, some of the radiation is transmitted through the sample and some is scattered by the material. In the particular case of semicrystalline polymers, X-ray scattering arises as a result of fluctuations in electron density associated with the stacking of dense polymer crystals and less dense amorphous interlayers. While x-rays are scattered by electrons, significant observable scattering can only be observed if a particular relationship exists between the magnitude of the scattering vector (a function of both the radiation wavelength and the scattering angle) and the length scale of these electron density fluctuations. Typical SAXS experiments readily allow the determination of periodicity in the structure of a material when such periodicity is in the range of 2 to 80 nm. SAXS experiments can be used to determine the average thickness of lamellar crystals assuming that the two phase model of semicrystalline polymers is valid and that the totality of the amorphous fraction is located between crystalline lamellae. In recent years the two-phase model has been refined through consideration of the crystal/liquid interphase. If polymer morphology is indeed comprised of three phases (crystal, amorphous and interphase), the

thickness of both crystalline and amorphous phases may be slightly overestimated if calculated on the basis of the two-phase model. In the second part of this thesis, small-angle x-ray scattering data of bisphenol A polycarbonate will be collected and analyzed in the context of the two-phase model.

Combination of these scattering data with results obtained from differential scanning calorimetry will allow us to probe a well-known correlation between the thickness and the melting temperature of semicrystalline polymers in the case of bisphenol A polycarbonate. This correlation, expressed by the Gibbs-Thomson equation, will allow us to obtain an estimate of the equilibrium melting temperature and fold surface free energy for this polymer.

Finally, an attempt will be made to compare the morphology of a bulk-crystallized polymer with the morphology of a thin polymer sample, to enable a comparison of their physical properties.

Chapter 2. Literature Review

2.1 Initial Stages of Crystallization

The induction period for an isothermal crystallization process is the time span between temperature equilibration and the onset of primary crystallization. The length of the induction period depends on the polymer and the crystallization conditions. It is generally observed that the induction period for a given polymer increases with the half time of crystallization. A number of studies over the last ten years have focused on the initial stage of crystallization, i.e. the induction period, and on the mechanism of homogeneous nucleation. Specifically, a number of researchers have questioned the validity of the theory of classical nucleation, suggesting that a preordering of sections of polymer chains may be occurring prior to primary nucleation. The results of a number of these investigations have suggested that during the induction period such preordering follows similar kinetic laws to these encountered during the spinodal decomposition of binary mixtures. The preordering process was compared to the nematic ordering of liquid crystalline polymers observed subsequent to cooling from the isotropic phase.

Research into the possible ordering during the induction period has been focused on three polymers, poly(ethylene terephthalate), isotactic polypropylene, and isotactic polystyrene. These three polymers were chosen because of their wide industrial applications. Imai et al. studied the induction stage of poly(ethylene terephthalate) with depolarized light scattering, small-angle X-ray scattering, and wide-angle X-ray diffraction.[8,9,10] Light scattering was used to detect both orientation and density fluctuations on a length scale of 0.1 to 50 μm, while small-angle X-ray scattering was

used to follow density fluctuations on the nanometer length scale. Wide-angle X-ray diffraction was used as a complimentary experimental technique to demonstrate that the onset of fluctuations in density and in orientation preceded the onset of primary crystallization. In summary, SAXS experiments showed the growth and shift to smaller scattering angles of a scattering peak with increasing annealing time during the induction period. Wide angle X-ray diffraction showed no evidence of crystalline order during the induction period. These results suggest that density fluctuations occur prior to primary crystallization. Light scattering results showed that there is an exponential increase in the total integrated intensity, i.e. the invariant, with annealing time, indicative of the parallel ordering of sections of polymer chains during the induction period. Small-angle X-ray scattering experiments suggest the growth of density fluctuations with annealing time within the induction period, and light scattering experiments suggest an exponential increase in orientation fluctuations with annealing time during the induction period. Both of these experimental observations are characteristic features of a spinodal decomposition mechanism. An increase in density fluctuations and orientation fluctuations, if real could suggest an ordering (without crystallization) of polymer chain segments during the induction period. This ordering process would exhibit a kinetic law consistent with what has been observed previously in systems undergoing spinodal decomposition. The authors, therefore, concluded that a pre-ordering process with kinetics identical to that observed for spinodal decomposition occurs prior to nucleation and growth. Imai et al. also employed small-angle neutron scattering to observe the changes in persistence length of the polymer chains during the induction period.[10] An increase in persistence length

with annealing time led to the conclusion that a "stiffening" of the chain conformation leads to a better local packing of sections of these chains prior to nucleation.

In a study of isotactic polypropylene, small-angle X-ray scattering and wide-angle X-ray diffraction were again employed and within an induction period of 400 seconds, the results were similar to those found by Imai et al. Terrill et al. used time-resolved SAXS/WAXD experiments so they could observe the evolution of the SAXS pattern while they simultaneously monitored the level of crystallinity by WAXD.[11] The change in the SAXS pattern during the induction period was consistent with a spontaneous increase in density fluctuations before the onset of crystallization. When the onset of crystallization was detected by WAXD, the SAXS peak shifted to higher values of the scattering vector, that are typical of those observed for stacks of lamellar crystals and interlamellar amorphous regions. Another study was performed with poly(ether ketone ketone) using simultaneous SAXS and WAXD.[12] Poly(ether ketone ketone) was chosen because it exhibits high chain stiffness, making it less mobile when heated above T_g. Even with the reduction of conformational mobility, the scattering results suggested the similar pre-ordering phenomenon during the induction period.

Despite the similarity in the experimental observations and in the conclusions reached for these different polymer systems, these studies met a great deal of skepticism from the scientific community.[13,14] Indeed, a number of factors were not considered in these studies, which could dramatically affect the conclusions drawn from the reported data. First and foremost, one must realize that polymer chains in a given polymeric material are usually not of identical length. This may be especially important for the three cases discussed above. The length of a polymer chain affects its flexibility especially in

the case of PEKK and PET since these materials are usually prepared in low molar mass. Spontaneous liquid-liquid phase separation of chains on the basis of stiffness, thus molar mass can account for the density fluctuations observed in the polydisperse polymer melt. These fluctuations could give rise to small-angle X-ray scattering patterns as the electron density of polymer chains depend on the chain length. Shorter chains exhibit a larger number of chain ends per unit volume, thus have higher free volume and lower density than longer chains. Liquid-liquid phase separation in polymer mixtures when spontaneous also follows a spinodal decomposition mechanism and kinetics. The afore-mentioned studies on poly(ethylene terephthalate), poly(ether ether ketone) and polypropylene used samples with polydispersity indices of 2.5, 2.0 and 4.44, respectively. Because of the significant breadth of these molar mass distributions, one could easily envision the existence of density fluctuations on the simple basis of liquid-liquid phase separation.

Polyethylene with a narrow molecular weight distribution was used to study the effect polydispersity may have on the induction period. There were no detectable changes in the SAXS peaks prior to the appearance of WAXD patterns for polyethylene samples with a polydispersity of 1.1.[13] Because of the lack of change in the SAXS pattern during the induction period, the authors concluded that no pre-ordering occurs, and nucleation follows classical nucleation and growth theory. In a later paper, the authors used polyethylene samples of significantly higher polydispersity, observed an evolution of the small-angle X-ray scattering pattern prior to the onset of crystallization detected by wide-angle X-ray diffraction and concluded that the proposed ordering

process during the induction period results from the effects of molecular weight and molecular weight distribution on the crystallization kinetics.[14]

One experimental difficulty shared by all studies mentioned above is that each of the polymers studied exhibits a fast rate of crystallization. High crystallization rates lead to short induction periods, which prevent a thorough examination of processes occurring during that period; the polymers mentioned in these previous studies had induction periods on the order of minutes. In order to study the induction period more rigorously, polymers with induction periods longer than a few minutes should be studied. In this project, bisphenol A polycarbonate was selected because it exhibits induction periods of at least a few hours, and its crystallization occurs so slowly that it can be quenched very effectively, without undergoing further crystallization. Since polycarbonate has only one crystal structure, the crystallinity and structure can be frozen and thoroughly studied. Two experimental techniques, differential scanning calorimetry and infrared spectroscopy, will be employed along with the common small-angle X-ray scattering and wide-angle X-ray diffraction. Differential scanning calorimetry will provide an accurate measure of the induction period by revealing the development of crystallinity as a function of annealing time. Infrared spectroscopy will provide information as to the existence of conformational changes of the polymer chains as a function of temperature or time. Combination of these four experimental techniques and the slow crystallization kinetics will allow conclusions to be drawn as to whether a preordering process can be observed during the induction period of bisphenol A polycarbonate.

2.2 Morphology

2.2.1 Isothermal Lamellar Thickening

As discussed in the Introduction, four different mechanisms have been proposed for secondary crystallization. Isothermal lamellar thickening is the process in which lamellae formed during primary crystallization increase their thickness during annealing to lower their surface to volume ratio. Since the basal planes of lamellar crystals (chain fold surface), exhibit a higher surface free energy than the lateral sides of the crystal, the thickening process leads to a stabilization of the crystal (decrease in free energy). The spontaneous evolution of chain folded lamellae during thickening should be simply viewed as an attempt by the lamellar crystals to reach the equilibrium state characterized by fully extended chain structures (i.e. with no fold). A survey of the literature suggests that isothermal lamellar thickening is only possible for the few flexible chain polymers characterized by a small repeat unit, such as polyethylene, polyethylene oxide, polypropylene, poly(tetrafluoroethylene). On the basis of molecular mechanics calculations, it was indeed speculated that isothermal lamellar thickening should not be observed in the case of polymers exhibiting large side groups, large repeat units or stiffer linkages, as the free energy for motion of conformational defects would be too large for such material. Without significant motion of conformational defects in a crystal, it is indeed difficult to envision the thickening of polymer lamellae. These calculations were however carried out using force field parameters describing the structure of polymer crystals at low temperature. One could expect that as a polymer crystal is heated toward its melting temperature and undergoes significant lattice expansion, the average interchain distances increase, facilitating motion of conformation defects within the

crystal lattice. Recent investigations of the secondary crystallization process have shown that, despite all expectations, the isothermal lamellar thickening process is indeed possible for polymers such as PEEK, PET, it-PS and BAPC.[6] Specifically, Alizadeh et al. showed the existence of a crossover phenomenon for secondary crystallization from secondary crystal formation at low temperatures to isothermal lamellar thickening at high temperatures.[6] The crossover temperature was evidenced through measurements of the rate of shift of the melting temperature with logarithm of crystallization time for different crystallization temperatures. The rate of shift of the melting temperature with time decreases with annealing temperature for temperatures below the crossover temperature, but above this temperature, the rate of shift increases with annealing temperature, which is consistent with lamellar thickening. Two supporting factors have been given to justify the possibility of lamellar thickening during annealing at high temperatures. The first is that polymer crystals are less dense at higher temperatures. Polymer chains in the crystalline phase have thus increased mobility so local changes in segmental conformation can take place, which can give rise to an increase lamellar thickness, thus a decrease in crystal free energy. Secondly, as the annealing temperature increases, the critical primary nucleus size and the lamellar thickness of minimum stability increase. When annealing temperatures are higher than the crossover temperature, the thickness of amorphous layer between lamellae may not be large enough to allow for the formation of new crystals or the sequence of polymer segments available for crystallization in the interlamellar amorphous fraction may be too short to form a stable crystal between the primary lamellae. The crossover behavior of bisphenol A polycarbonate was demonstrated by Alizadeh et al. and is shown in Figure 4 (crossover temperature is 213°C

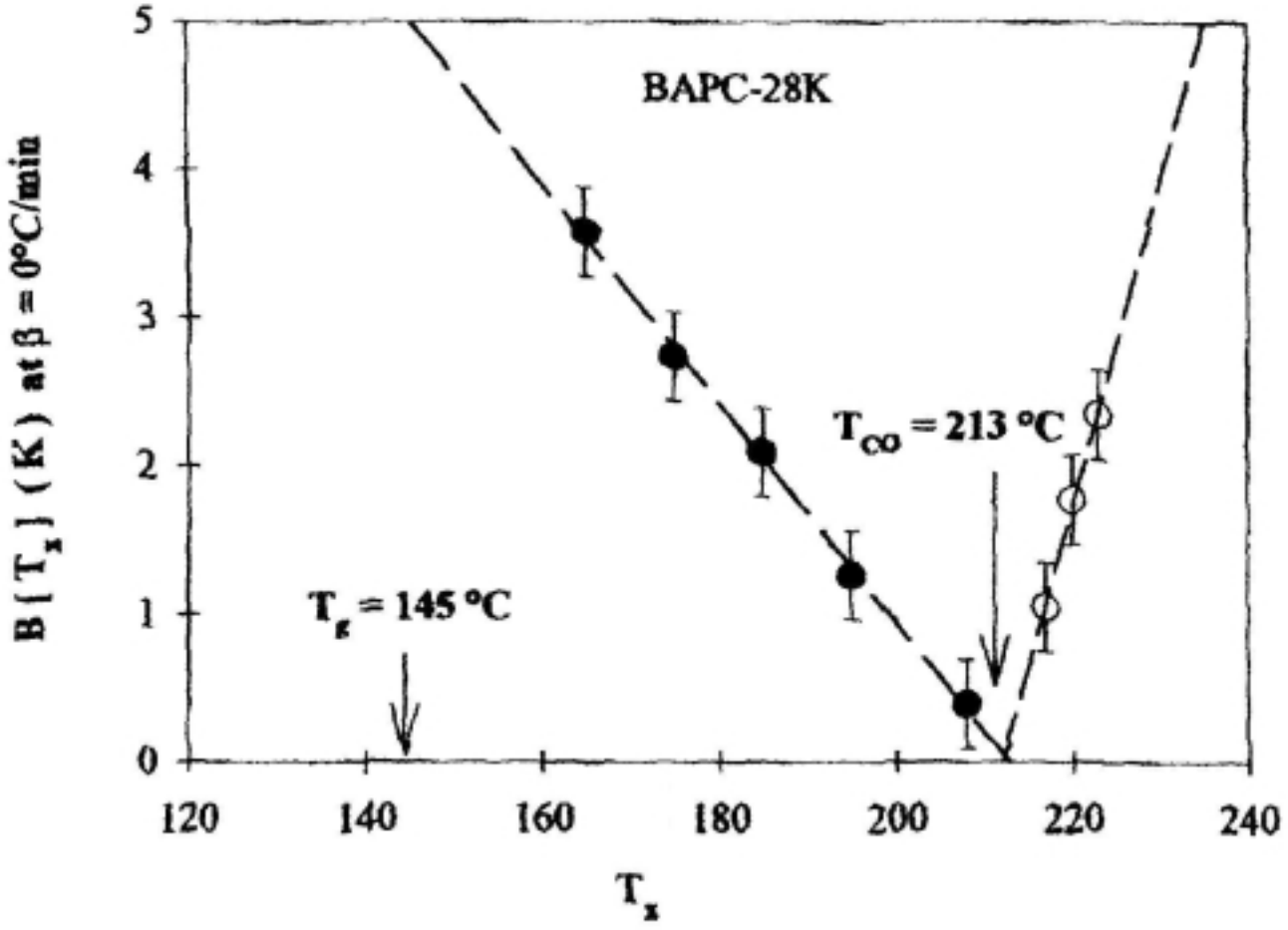

Figure 4. Rate of Shift of the Low Endotherm as a Function of Crystallization Temperature for 28,000g/mol Polycarbonate

for a sample of weight average molar mass equal to 28,000 g/mol). Other polymers, including poly(ethylene terephthalate) (PET), poly(ether ether ketone) (PEEK), and isotactic polystyrene (it-PS), have shown similar crossover behavior and are also expected to exhibit lamellar thickening at temperatures above this crossover temperature.

The thickness of a lamellar crystal can be correlated to the melting temperature of that crystal by the Gibbs-Thomson equation:

$$T_m = T_m^0 \left[1 - \frac{2\sigma_e}{\Delta H_f^0 \ell_c} \right] \quad \textbf{(6)}$$

where σ_e is the fold surface free energy, ΔH^0_f is the enthalpy of fusion for a perfect crystal, T^0_m is the melting temperature of an infinitely large and perfect crystal, and l_c is the lamellar thickness. As a polymer crystal thickens with annealing time, the melting temperature of the polymer will increase, approaching T^0_m. This relationship has been verified by the study of various polymers, including polyethylene[5] and isotactic polypropylene[15]. Many studies use the relationship between lamellar thickness and melting temperature to determine the surface free energy and equilibrium melting temperature of the polymer.

Polycarbonate is a semiflexible polymer that has been shown to follow isothermal lamellar thickening in two previous studies.[6,16,17] Because polycarbonate experiences thickening with annealing time, the authors were able to show that polycarbonate followed the trend of the Gibbs-Thompson equation. The results from these two prior studies on polycarbonate are well correlated and indicate, in agreement with the Gibbs-Thomson equation, that the melting temperature of BAPC lamellae decreases linearly

with the reciprocal of the lamellar thickness. However, the limited amount of experimental data points leads to rather large uncertainties in the estimation of the fold surface free energy and equilibrium melting temperature for polycarbonate. Jonza et al. reported a surface free energy a 70 mJ/m^2 and an equilibrium melting point of 335°C [16], while Sohn reported values of 52 mJ/m^2 and 324°C, respectively.[17] In light of this rather large spread in the estimated thermodynamic parameters, further investigation of bisphenol A polycarbonate is warranted. It should also be noted that while the results obtained by these two groups compare favorably with each other, the experimental approach followed by Sohn is dramatically different from that used by Jonza et al. Specifically, Sohn study the morphology and melting behavior of thin films using atomic force microscopy, while Jonza et al. used bulk samples and the small angle X-ray scattering technique.

2.2.2 Lamellar Thickness Determination

2.2.2.1 Small-Angle X-ray Scattering

The most common technique for lamellar thickness determination is small-angle X-ray scattering. Small-angle X-ray scattering measures the periodicity of electron density fluctuations between ordered (crystalline) and disordered (amorphous) regions in a semicrystalline sample. Results from small-angle X-ray scattering experiments have to be thoroughly analyzed to extract useful data, such as the lamellar crystal thickness and the amorphous layer thickness. A number of methods have been proposed for the estimation of lamellar thicknesses by small-angle X-ray scattering, namely Bragg's law and the correlation and interface distribution function approaches.

In all cases, a number of corrections have to be applied to the raw scattering data before any of these analyses can be carried out. The first correction is concerned with the subtraction of the parasitic scattering (or empty beam scattering). It must be carried out accounting for the absorption of the X-ray beam by the polymer sample. Absorption factors calculated from density, composition and atomic absorption factors and measured experimentally for each of the samples agreed with each other within the experimental uncertainty. The second correction, called the Lorenz correction, accounts for the fact that the scattering of an isotropic semicrystalline polymer while recorded between scattering vectors q and q+dq, is actually distributed over a corona of radius q and thickness dq in the plane of the detector. The total scattering intensity, I(q), at a given scattering vector q is therefore obtained by multiplying the scattering intensity at q by the term $4\pi q^2$ as shown bin Equation 7.

$$I(q) = 4\pi q^2 I_0(q) \tag{7}$$

where I_0 is the input data from the experiment, and the scattering vector is defined as:

$$q = \frac{4\pi}{\lambda}\sin(\theta) \tag{8}$$

where 2θ is the scattering angle and λ is the wavelength of the x-ray radiation. The scattering curve is also extrapolated to zero scattering vector, a correction that is only necessary if the scattering intensity is used to estimate the correlation function or the interface distribution function.

In a plot of the corrected data, I(q) vs. q, a single peak appears at the scattering vector denoted q_B. This scattering vector can be used in the Bragg law to yield the length scale associated with the periodicity in electron density fluctuation. This periodicity is called the long spacing, L_B, and is defined as the sum of lamellar crystal thickness and amorphous phase thickness. An average thickness of the lamellar crystalline phase, l_c, is obtained by multiplying the long spacing by the volume fraction crystallinity of the bulk sample, which can be determined from wide-angle X-ray diffraction, dilatometry or differential scanning calorimetry. For this analytical approach to have any merit, the volume fraction crystallinity of the bulk polymer sample must be equal to the local volume fraction crystallinity associated with the stacks of crystals and amorphous layers. Assuming that bulk and local crystallinity are identical is equivalent to the assumption that there is no amorphous regions outside the lamellar stacks.

The second method for determining the lamellar thickness considers the correlation function. The correlation function, $\gamma(r)$, is the Fourier transform of the Lorenz corrected scattering curve. Equation 9 shows the expression for the one dimensional correlation function.

$$\gamma(r) = \frac{\int_0^\infty I(q)\ q^2 \cos(qr)\, dq}{\int_0^\infty I(q)\ q^2\, dq} \qquad \textbf{(9)}$$

The data that are input into the correlation function must be extrapolated to low and high scattering angle. The extrapolation for low q, which is of relatively minor importance as it is concerned with structural information on very large length scales (much larger than the long spacing), is performed using a linear function of the scattering vector. The

extrapolation to high q is not only much more complicated but it is also much more important as it is concerned with information on a length scale commensurate with the thickness of amorphous and/or crystalline layers. For a two-phase system with a sharp interphase and no electron density fluctuation within each phase, the scattering intensity at high q should follow the Porod law.

$$I(q) = \frac{K_P}{q^4} \tag{10}$$

There are however two phenomena which contribute to scattering in the Porod region and which lead to deviation from the Porod law. First, the existence of an interphase (interface of finite thickness) between crystal and amorphous layers, leads to a gradient in electron density between crystal and amorphous regions, decreasing the intensity predicted by the Porod law. Second, density fluctuations exist within each phase, but predominantly within the amorphous phase. These density fluctuations lead to an increase in scattering above that expected from the Porod law. This liquid scattering, actually, can be viewed as the low q branch of the amorphous halo observed in wide angle X-ray diffraction experiments. Verma et al. found that variation of the constants (within reasonable bounds) describing the crystal-liquid interphase profile and the liquid scattering only affected the final results by 5%.[18] Subsequent to extrapolations to high and low q and Fourier transformation of the scattering profile, one obtains the correlation function. Analysis of the correlation function leads to the estimation of two length scales l_1 and l_2, the former being conventionally the lowest value. Because of the Babinet reciprocity principle, it is impossible to infer from analysis of the scattering profile with the correlation function which of these two length scales correspond to the crystal

thickness and which corresponds to the amorphous layer thickness. Indeed, there has been and still is much debate on this issue and on the associated issue of whether local and bulk degrees of crystallinity are identical. This controversy is especially important in the case of polymers of low degree of crystallinity. If the bulk degree of crystallinity is low, the value of the crystal thickness determined by multiplying long spacing by crystallinity is similar to the lower value, l_1.[19] This assignment is therefore consistent with the assumption that bulk and local crystallinities are identical. On the other hand, if the higher (l_2) of the two values obtained from the correlation function is taken as the lamellar thickness, then the local crystallinity is found to be larger than the bulk crystallinity, suggesting the existence of large amorphous regions between stacks of lamellae. If these amorphous regions are large enough, they will not contribute to the scattering profile in the angular range associated with the long spacing. One anticipates that during isothermal lamellar thickening, only one of the two length scales should increase with time. The length scale that increases must be associated with the lamellar thickness.[19]

Even though small-angle X-ray scattering is the most widely employed technique for lamellar thickness measurements in polymers, the above discussion makes it clear that the analysis of such data is ambiguous, especially, in the case where scattering data is collected in an angular range that is too small to correct the scattering curves for deviations from the Porod law. Unfortunately, this was the case in our study, so the scattering curves are only analyzed using the Bragg law under the assumption that local and bulk crystallinities are identical. Direct observations of the morphology by microscopy techniques could then be used to evaluate long spacing and lamellar

thickness and thus allow independent evaluation of the assumptions used to analyze the small angle X-ray scattering data.

2.2.2.2 Microscopy

Since the determination of lamellar thickness by small-angle X-ray scattering requires numerous assumptions and extrapolations, it is worthwhile to look at other experimental techniques as a means of obtaining the lamellar thickness for a polymer sample. A direct measurement, by observing the actual morphology of the sample, would seem to be the best way to measure lamellar thickness. Techniques such as atomic force microscopy, scanning electron microscopy, and transmission electron microscopy are potential methods for directly measuring lamellar thickness. Various polymer morphologies have been examined with the mentioned microscopy techniques, but special preparation procedures must be followed for these experiments. Polymers films must be stained or etched to increase contrast and help estimation of the lamellar thickness. Bulk samples must be microtomed to create a thin section for transmission electron microscopy. In each microscopy technique, the bulk structure may be altered in order to observe the morphology of the polymer sample. These alterations could lead to errors in the measurement of lamellar thickness. A comparison between three microscopy techniques used to determine lamellar thickness (SAXS, TEM, and AFM) found that the results from TEM and SAXS were in good agreement, but thickness values measured by AFM were approximately 14% larger.[20] These results may be due to the difference in structure between the surface of a sample and the bulk of the sample. A second reason for the overestimation may be that in a bulk material, the lamellae can be

oriented in any direction at any angle, whereas the orientation of lamellae at the surface are perturbed by the surface itself.

2.2.3 Epitaxial Growth

If polymer crystals can form edge-on on a substrate, the lamellar thickness can be directly measured. If there is no crystallographic relationship between the polymer and the substrate, the morphology of the polymer will be random. If there are crystallographic relationships between the polymer and substrate, the polymer lamellae may orient in unique direction with respect to the substrate.

Epitaxy is the growth of a crystalline phase on a crystalline substrate, yielding a specific structure or orientation of the growing crystal. Two types of polymer epitaxial growth can occur, fold plane and fold surface epitaxy. Fold surface epitaxy is the unusual growth of the polymer lamellae with the folded surface parallel to the substrate. The classical form of epitaxy, fold plane, involves the polymer chain axis orienting parallel to the substrate creating edge-on lamellae. The first study of epitaxial growth was performed with polyethylene on the surface of sodium chloride. An oriented morphology was observed with optical and electron microscopy.[21] To create an edge-on orientation of lamellae, a few specific conditions must be fulfilled, as not all polymers and substrate combinations will result in epitaxial growth. The most important condition for epitaxy is that the interchain distance must match a periodicity in the substrate within 15%, i.e. aspects of the unit cell periodicity must match.[21] For organic substrates such as a polymer, the periodicity is the interchain distance, whereas the periodicity of an inorganic substrate such as alkali halides is the atomic spacing. Since the chains lay flat

on the surface, the lamellae will grow on edge displaying the alternating crystalline and amorphous phases. Observing the lamellae edge-on allows the determination of the lamellar thickness by a direct measurement, but the results may be difficult to compare to these obtained from samples crystallized in the bulk, because epitaxially crystallized films are typically very thin, so that the crystallographic memory associated with epitaxy is not lost during growth normal to the substrate. Film thickness effects may lead to differences in morphology.

The epitaxial crystallization of bisphenol A polycarbonate on Iceland Spar calcite has already been studied because two of the calcite unit cell dimensions provide a relatively good match for one of the interchain distances found in bisphenol A polycarbonate crystals.[17] Sohn grew crystals by an isothermal crystallization process and observed them using atomic force microscopy. Results showed that only pseudo epitaxy occurred with sections of the crystal being nearly perpendicular to the substrate.[17] Another study of polycarbonate epitaxy was discussed by Wittmann et al.[22] Bisphenol A polycarbonate crystals were found to grow epitaxially on two aromatic organic substrates, anthracene and *p*-terphenyl. The epitaxially-grown crystals were formed from a polycarbonate/p-terphenyl mixture at a high temperature. The polymer and organic materials phase separated as the mixture was cooled from the initial temperature, yielding a p-terphenyl substrate upon which the polycarbonate crystallized epitaxially.[23]

Chapter 3. Experimental

This chapter details the preparation and characterization of samples, and the various experimental procedures that were employed in this project. Bisphenol-A polycarbonate, trade name Lexan, of 19,000 weight average molar mass was used as-received from GE in pellet form.

3.1 Sample Preparation

3.1.1 Bulk Sample Preparation

Polycarbonate pellets were molded into square or circular shaped plaques in a Carver Laboratory press by heating to 260°C under an inert nitrogen purge with a pressure of 10 kPa. Circular samples for small angle x-ray scattering experiments were 1 mm thick and 25 mm in diameter. Square samples for calorimetry experiments were approximately 0.5 mm thick and 50 mm on each side.

3.1.2 Thin Films Preparation

Thin films were solution cast onto three different substrates for epitaxial crystallization: 5 mm^2 pieces of cleaved Island Spar calcite (Ward Scientific), silicon wafers (Wacker Siltronic), and 22 mm diameter glass coverslips (Chance Proper Ltd.). A 5 wt/wt % solution of bisphenol A polycarbonate in chloroform was initially prepared for dip-coating the calcite and glass substrates. For epitaxial growth, films must be extremely thin, on the order of 100 nm, so thickness variations caused by dip coating had to be avoided. The silicon wafer and glass coverslips were spin coated at room temperature with a 2 wt/wt % solution at speeds of 2000 and 3000 rpm.

P-terphenyl was used as a fourth substrate for the epitaxial crystallization of bisphenol A polycarbonate. Single crystals of the organic material were prepared by two methods. The p-terphenyl powder was found to sublime at approximately 200°C. Sublimation led to crystals approximately 1 mm across. Single crystals were also grown from a 10 wt/wt % solution of p-terphenyl in diethyl ether. As the solvent evaporated, single crystals on the order of 1 mm across were formed. These crystals were sandwiched between a glass slide and polycarbonate films to induce epitaxial crystallization on the polymer surface upon heating the initially amorphous above its glass transition temperature. This process of epitaxial growth was unsuccessful because the p-terphenyl either sublimed prior to crystallization at a temperature of 190°C, or the polymer film could not be separated from the glass slide after crystallization.

3.1.3 Crystallization

Differential scanning calorimetry studies of bisphenol A polycarbonate of different molar masses have been previously studied.[17] These studies enabled the determination of crystallization half time (i.e. the time necessary to achieve half of the maximum crystallinity), for different crystallization temperatures. Figure 5 is a plot of crystallization half time as a function of crystallization temperature. The shortest half time occurs near a temperature of 190°C for all molecular weights examined; therefore, to optimize the crystallization process, samples in the present work were crystallized at 190°C in a Blue Oven™ under dry nitrogen flow.

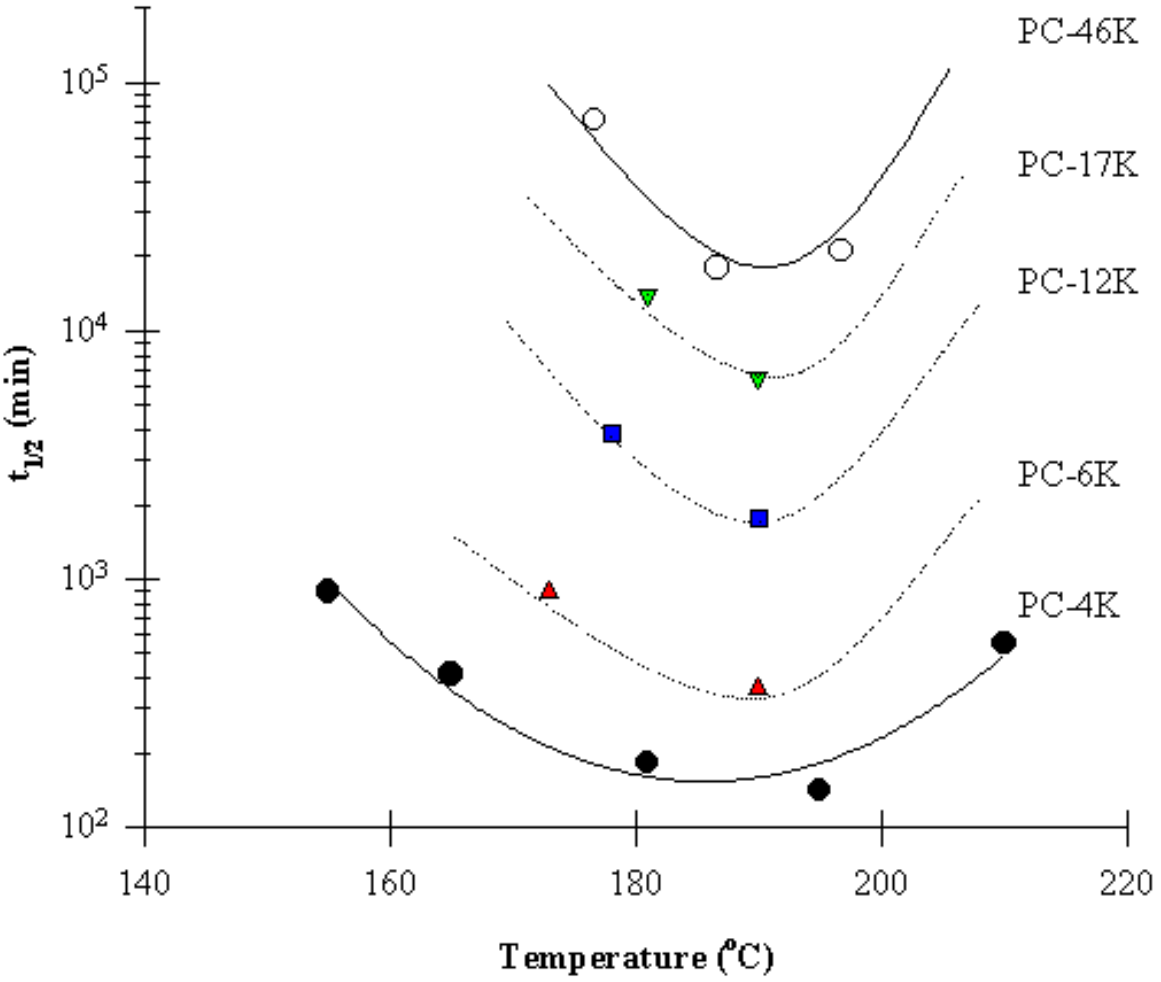

Figure 5. Crystallization Half Time as a Function of Crystallization Temperature for Various Molecular Weights of Polycarbonate[13]

3.1.3.1 Studies of Initial Stages of Crystallization

Samples for the determination of the induction period for crystallization were prepared by crystallization at 190°C for times ranging from 30 minutes to 10 hours. One set of samples was prepared for investigations of the degree of crystallinity and density fluctuations using three different experimental techniques (SAXS, WAXD, and DSC). Since the process of crystallization is highly dependent on the actual temperature, the molar mass, and concentration of impurities, use of a unique set of samples eliminates the possibility of inconsistency between experiments due to sample variation.

3.1.3.2 Studies of Lamellar Thickening

Since samples used in the lamellar thickening studies required a high degree of initial crystallinity, they were crystallized for 8 days at a temperature of ~190°C (some variation in the oven's temperature control were noted). The samples were then quenched to room temperature and placed in an oven at an annealing temperature above the initial crystallization temperature. Two sets of samples were prepared. One group was annealed at 223°C and the other was annealed at 228°C. Samples annealed at 228°C were crystallized and annealed in evacuated tubes to reduce the possibility of chemical degradation at the higher annealing temperature. All samples were quenched with air upon their removal from the oven and were kept subsequently in a dessicator to eliminate the uptake of water.

3.2 Experimental Procedures

Although two different studies were performed on bisphenol A polycarbonate, the experimental procedures were very similar and each technique will be described in general, with variations between the two studies identified within the general section.

3.2.1 Differential Scanning Calorimetry

The thermal behavior of bisphenol A polycarbonate samples was studied using differential scanning calorimetry. A Perkin Elmer Pyris differential scanning calorimeter was operated with a dry nitrogen purge and an ice/water bath for measurements of heat flow as a function of temperature. A baseline was established for the instrument using two empty aluminum DSC pans. This baseline allows for the correction of heat flow variation due to the equipment by subtracting the baseline heat flow from the sample heat flow. Samples of mass 10 ± 2 mg were sealed in DSC pans and heating traces were recorded from 100° to 250°C at a rate of 10°C/min. Temperature and heat capacity calibrations were performed with pure metal standards. The temperature calibration was performed using an pure indium standard, run from 100° to 250°C at various heating rates. Extrapolation of the indium melting temperature to zero heating rate and comparison with the actual reported melting temperature allowed the DSC temperature scale to be calibrated. The heat capacity calibration was performed using sapphire, which has a known heat capacity for a given heating rate. The sapphire standard was heated under the same conditions as the bisphenol A polycarbonate samples. Comparison of the experimental heat capacity of sapphire measured at different temperatures with the tabulated theoretical values allowed calibration of the heat flow rate in the DSC.

3.2.2 Infrared Spectroscopy

The equipment employed for infrared spectroscopy experiments was a Bio-Rad Fourier-transform infrared spectrometer with a heating device attached for isothermal holding at the crystallization temperature. The spectrometer detector was cooled with liquid nitrogen, and the system was purged with nitrogen gas to eliminate water, which could affect the spectra recorded.

The heating device was calibrated using a polyethylene sample because two peaks in the rocking region of the polyethylene spectrum disappear as the melting temperature of the polymer is reached. Scans of the polyethylene were taken at various temperatures from room temperature to 130°C, after which scans were taken every degree. The melting point was taken as the temperature at which the doublet in the rocking region transforms to a single band. Comparison of the temperature determined from the disappearance of the doublet to the melting point of polyethylene measured by differential scanning calorimetry allowed calibration of the temperature scale of the heater.

A background spectrum was recorded with two salt (KBr) plates in the optical path. This was used to account for equipment variations during experimentation, similar to baselines described for calorimetry experiments. A thin film of polycarbonate, on the order of 40μm thick, was sandwiched between the KBr plates, and the temperature was raised to 190°C for crystallization. Spectra were taken at various time intervals, ranging from ten minutes to thirty minutes, over five and a half hours. One sample was crystallized in the Blue Oven™ for approximately four days so

that the infrared spectrum of a well-crystallized sample could be recorded for comparison to samples crystallized for short times.

3.2.3 Small-Angle X-ray Scattering

3.2.3.1 Experiments

Small angle x-ray scattering was used to determine the lamellar thickness of the bulk crystallized polycarbonate samples. Experiments were performed using a Molecular Metrology small-angle X-ray scattering system with a 2-D area detector. Cu Kα radiation was obtained from a rotating anode generator operated at 45 kV and 70 mA. The exposure time for samples used for studies of the induction period was two hours. Samples for lamellar thickness measurements were exposed for one hour. Results were displayed in real time through the computer program MPANT.

Scattering angle calibration of the x-ray scattering camera was performed using the 54.2 nm d-spacing of duck tendon.[24]

3.2.3.2 Data Corrections

The MPANT program recorded the intensity at each pixel of the 1024 pixels by 1024 pixels 2-D area detector. Corrections of these data have to be performed to eliminate the effects associated with electronic noise in the detector, with parasitic scattering by the pinholes and beam stop or due to variation in sample thickness (i.e. absorption). Beam stop scattering causes high intensity flaring around the beam stop on the detector. To remove the effect of the flaring in sample patterns, the intensity of the x-ray beam without a sample, I_{blank}, was recorded. Electronic noise in the detector was corrected by measuring the dark current, which is the measurement of intensity with no

x-ray beam. The dark current intensity, I_{dark}, was subtracted from both the intensity of the sample(I_{samp}) and I_{blank} after the normalization for the timescale of each exposure (See Equation 11a and b).

$$I'_{samp} = \frac{I_{samp}}{sample\,time} - \frac{I_{dark}}{dark\,time} \quad \textbf{(11a)}$$

$$I'_{blank} = \frac{I_{blank}}{sample\,time} - \frac{I_{dark}}{dark\,time} \quad \textbf{(11b)}$$

where *sampletime* and *darktime* are the exposure times for the sample or blank and the dark current, respectively. After I_{blank} was corrected for the dark current, the data had to be corrected for absorption by the polymer. The intensity of the beam that strikes the detector with no sample is greater than if a polymer sample was in the beam path. The blank sample intensity is higher than I_{samp} by a factor defined as the sample absorption coefficient. The absorption coefficient was measured directly using the SAXS camera, as the ratio of the intensity with the sample in the beam, I, to the intensity without the sample, I_0, as shown in Equation 12.

$$I''_{blank} = I'_{blank} \times \frac{I}{I_0} \quad \textbf{(12)}$$

The resulting intensities (I''_{blank}) from the absorption coefficient multiplied by I'_{blank} were subtracted from I'_{samp}, which eliminates the contribution due to beam stop scattering. Finally, the data were corrected for changes in sensitivity across the area of the detector. Dividing the sample intensity by the sensitivity intensity (recorded using an isotropic ^{55}Fe

source), after normalization with the data acquisition time gave the scattering data corrected for all instrumental and sample variations.

A Fortran program was written to convert the two-dimensional scattering intensity data set into a more usable format. Since the samples are isotropic, the two-dimensional scattering patterns exhibit circular symmetry. The scattering intensities were circularly averaged to get a scattering profile (intensity as a function of distance from the center of the scattering pattern). The distance from the center, given in pixels, was changed to scattering angle using 1) the duck tendon calibration curve to convert pixels to meters and 2) the sample to detector distance, C, as shown in Equation 13.

$$2\theta = \tan^{-1}\left(\frac{r}{C}\right) \tag{13}$$

where r is the distance between a given pixel and the center of the two-dimensional scattering pattern. From the scattering angle, the d-spacing and scattering vector, q, were calculated by Equations 14 and 8, respectively.

$$d = \frac{\lambda}{2\sin\theta} \tag{14}$$

$$q = \frac{4\pi}{\lambda}\sin\theta \tag{8}$$

Intensity data were also averaged and corrected using a program created by Professor Dale Schaeffer from the University of Cincinnati. Using a subroutine in the analysis program Igor, the intensities from the sample, blank, sensitivity, and dark current runs were circularly integrated prior to the corrections described above. The sensitivity

file was masked to remove extraneous data around the beam stop and in the corners of the image plate. Adding a mask to the data eliminates the spurious and asymmetric scattering effect at very low scattering angles when the transmitted X-ray beam does not hit the center of the beam stop, which was unavoidable in most scattering experiments.

In all cases these scattering curves were then Lorenz corrected and the scattering vector at maximum scattering intensity was used to calculate the long spacing.

3.2.4 Wide-Angle X-ray Diffraction

Wide-angle X-ray diffraction experiments were performed on a Bruker AXS D8 Discovery diffractometer operated in reflection and the diffraction data was recorded using a 2-D image plate. Cu-Kα radiation was used, and the voltage and current were set at 40 kV and 20 mA, respectively. Samples were aligned in the beam, and the diffraction data was recorded using a 10 minutes exposure time. The data were analyzed using the General Area Detector Diffraction System (GADDS) and Diffraction Plus software provided with the Bruker system. The diffraction pattern was recorded from a 2θ of 5° to 35° over a constant azimuthal angle, where 2θ is the diffraction angle.

3.2.5 Synchrotron

Scattering experiments were also carried out at the X-27C beam line in the Brookhaven National Laboratory synchrotron center. The samples prepared to study the initial stages of crystallization were run using both wide-angle X-ray diffraction and small-angle X-ray scattering. Both sets of experiments were carried out with X-ray radiation of wavelength equal to 1.366Å. For wide-angle diffraction experiments, the sample to film distance was 171 mm. Small-angle scattering experiments were set up

with a sample to detector distance of 1660 mm. The exposure time for each sample was 30 seconds. Line scans were performed on the all diffraction and scattering patterns to extract data for further analysis.

3.2.6 Microscopy

Atomic Force Microscopy studies were performed on bulk crystallized polycarbonate samples using a Digital Instruments microscope in tapping mode. In atomic force microscopy, a silicon tip, attached to a cantilever, taps along the surface of the polymer, measuring 1) the difference between the phase of the set tip oscillation and the phase after the tip has come into contact with the sample, and 2) the height with respect to a set value. Samples were scanned over areas 2 μm to 5 μm across using a frequency of 1Hz.

The same samples used in small-angle X-ray scattering experiments were used for the AFM measurements. Imaging of the sample surface was attempted, but images of the polymer morphology were of poor quality, probably a result of sample preparation requiring the polymer to be pressed on a flat surface. In order to better image the morphology, the polymer was microtomed using an Ultracut Microtome from Reichert-Jung.

The surface morphology of bisphenol A polycarbonate was also studied after etching with diethylenetriamine and triethylamine. Etching agents remove the lower density amorphous material from the structure, exposing the crystalline lamellar structure. Scanning electron microscopy was employed to observe the etched surfaces of the bisphenol A polycarbonate. Because polymers generally do not conduct electricity, all polycarbonate samples were coated with a thin layer (3 nm) of palladium-platinum. A

LEO system field emission scanning electron microscope was employed, using an InLens detector, aligned perpendicular to the sample, to observe the sample's surface. A voltage of 5 kV was used for most micrographs, but the polymer was easily affected by the direct beam intensity, making it necessary to use 2 kV for some of the higher magnification images.

Chapter 4. Initial Stages of Crystallization

4.1 Results

4.1.1 Differential Scanning Calorimetry

Differential scanning calorimetry traces show the heat flow as a function of temperature during heating or cooling of a sample. First and second order transitions can be determined from DSC traces, because as the polymer goes through the transition, there is a change in heat flow. A first order transition, such as melting, is characterized by a peak in the heat flow vs. temperature curve, whereas a second order transition, such as the glass to rubber transition, is characterized by an a step increase in heat flow, the inflection point defining the glass transition temperature. For a sample crystallizable polymer heated from the amorphous state below the glass transition temperature, a DSC trace can exhibit a number of transitions: glass transition (step increase in heat flow rate), crystallization (exothermic process), and melting (endothermic process). Crystallization peaks are not observed during heating for polymers that exhibit fast enough kinetics of crystallization that they cannot be quenched to the amorphous state. Crystallization of a polymer, initially in the amorphous state at room temperature, requires heating the polymer above its glass transition temperature so there is sufficient molecular mobility to allow the conformational changes that are necessary for crystal formation. The rate of crystallization is then the result of a fine balance between the driving force for crystallization, which increases with undercooling, and the molecular mobility, which increases with temperature above T_g. As a result, the crystallization rate is a maximum at

a temperature between T_g and T_m and approaches zero as the temperature approaches the equilibrium melting or the glass transition temperatures. If the interval between the glass transition and the equilibrium melting temperatures is too narrow the maximum rate of crystallization can be very small, and the polymer may only crystallize if heated at a very slow rate or kept under isothermal conditions for long periods of time between T_g and T_m. This is the case for polymers such as bisphenol A polycarbonate.

Differential scanning calorimetry traces for polycarbonate samples crystallized at 190°C for various times are shown in Figure 6. The crystallization times range from 0 minutes (amorphous) to 10 hours, at which point crystallization should have begun. Data shown in Figure 6 could not be normalized due to equipment problems, so another set of samples was prepared and studied by differential scanning calorimetry. Experimental calorimetric data for the first set of samples are shown anyway since this unique set of samples is also used in the small-angle X-ray scattering and wide-angle X-ray diffraction experiments discussed later. Since the same trend is observed for both sets of samples, it is acceptable to use the second set of sample for analysis of the differential scanning calorimetry data.

The normalized heating traces are shown in Figure 7 for the second set of samples. Melting endotherms are only observed for crystallization times longer than 4 hours in this set of samples. As shown in the plot, for crystallization times under 5 hours, there is no evidence of heat flow evolution at temperatures in the temperature range expected for the melting of polycarbonate (~245°C), making all of the traces similar to that of the amorphous trace. After the fourth hour, the heat flow fluctuates with temperature, indicating the melting of polymer crystals. The heat flow is directly related

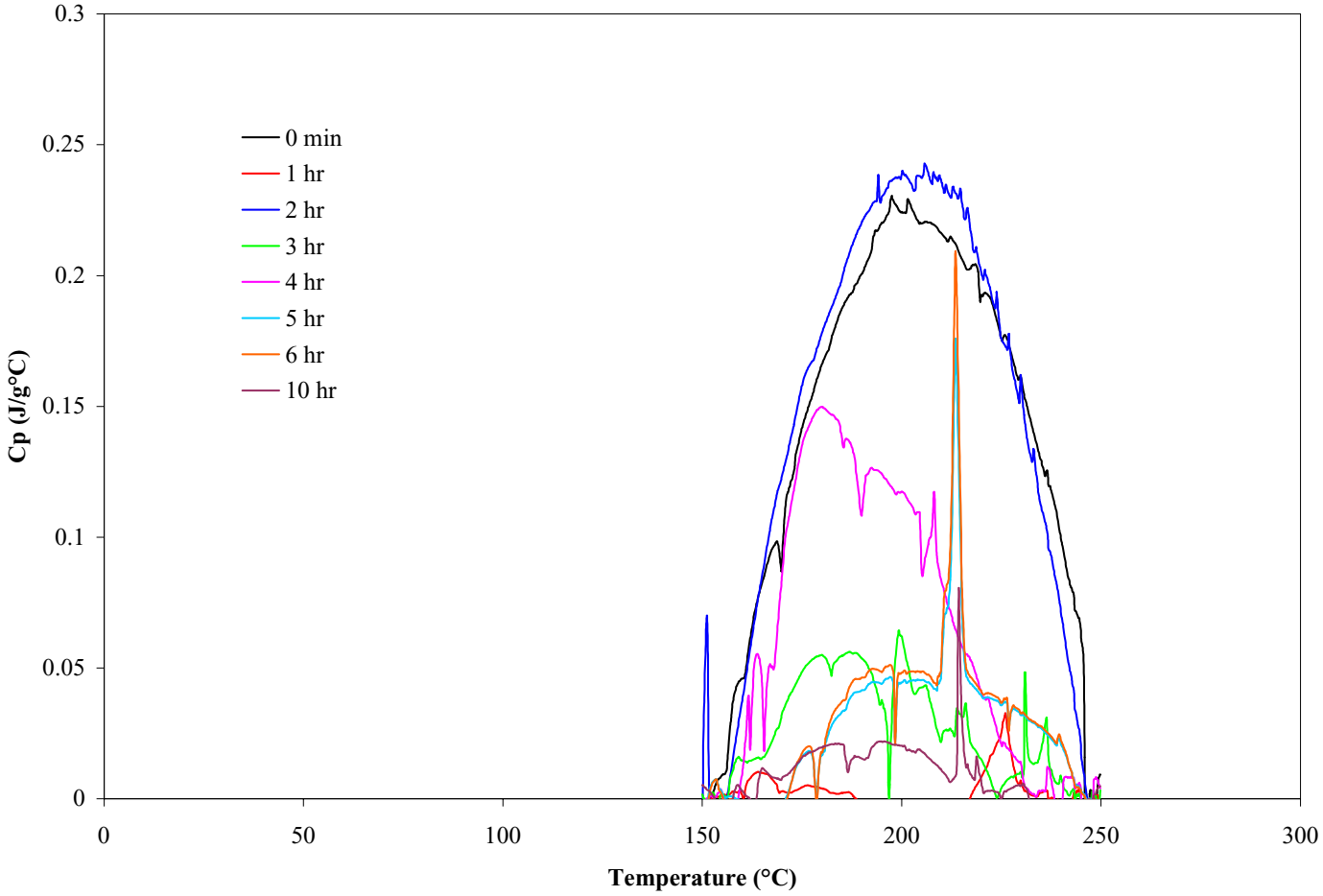

Figure 6. Differential Scanning Calorimetry Heating Traces of Polycarbonate Crystallized at 190°C for Various Times

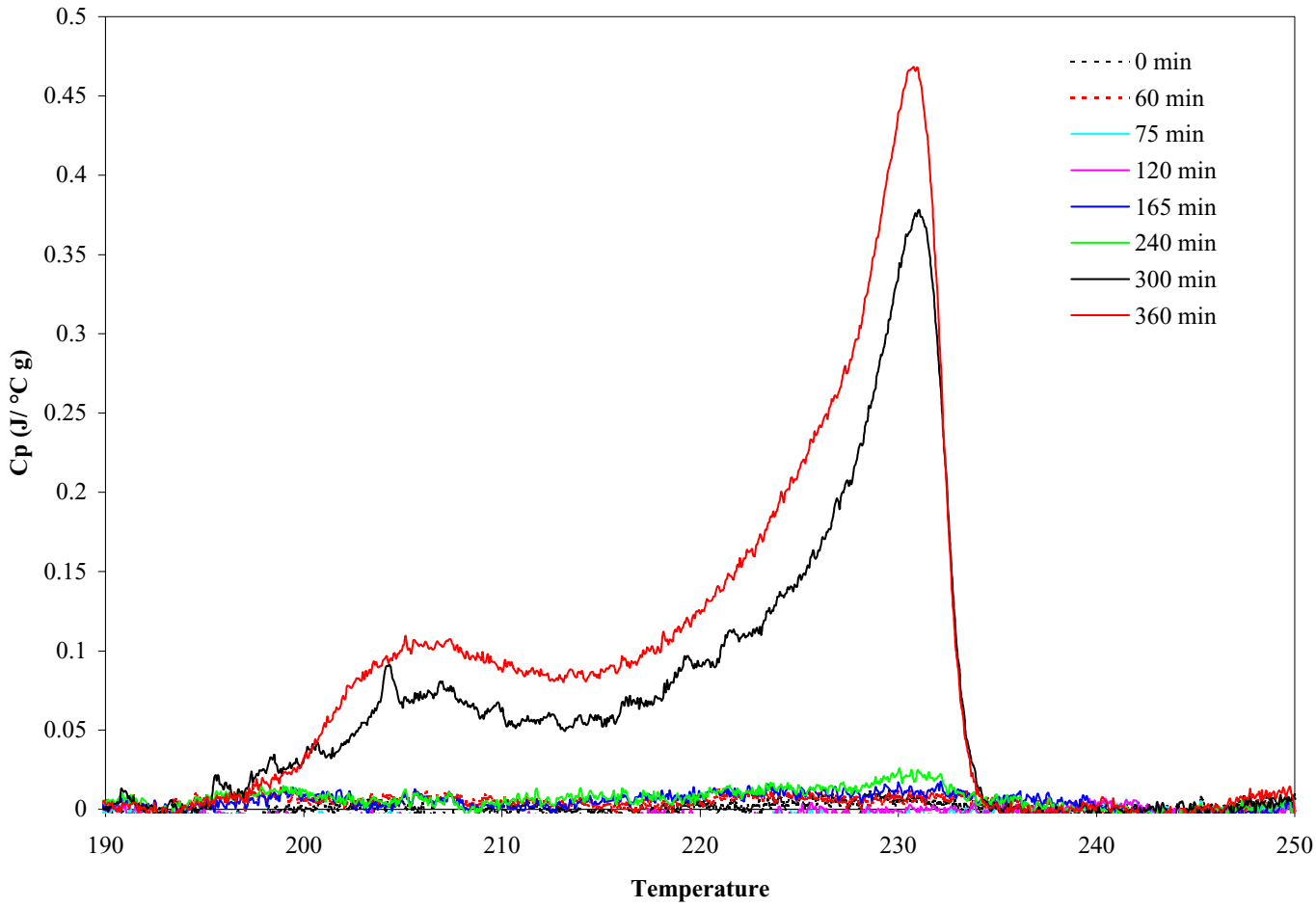

Figure 7. Normalized Heating Traces of Polycarbonate Crystallized at 190°C for Various Times

to the heat capacity by factors of the sample mass and heating rate (HR), as shown in Equation 16).

$$C_p = Heat\ Flow(mcal/\sec) \times \frac{4.18J}{1cal} \times \frac{60\sec}{1\min} \times \frac{1}{HR(^{\circ}C/\min)} \times \frac{1}{mass(mg)} \quad \textbf{(15)}$$

From the DSC traces, the heat of fusion of the sample can be calculated from the area under the curve of heat capacity vs. temperature. The heat of fusion calculated for each DSC trace is plotted in Figure 8 as a function of the crystallization time. As a result of the intrinsic sensitivity of the differential scanning calorimeter, detection of crystallinity less than 1% is not possible. After the fourth hour, the heat of fusion increases, indicating the beginning of primary crystallization. The induction period is defined as the crystallization time at which the heat of fusion begins to increase, and therefore, the induction period for polycarbonate crystallized at 190°C is taken as four hours for the remainder of this project.

4.1.2 Small-Angle X-ray Scattering

Small-angle X-ray scattering is a scattering technique that provides structural information for materials that have inhomogeneities (fluctuation in electron density) on the length scale of nanometers (10 – 1000 A). Polymer liquids, similar to every other liquid, exhibit density fluctuations. If the liquid is in thermodynamic global equilibrium, the density fluctuations should be independent of time. If, on the other hand, a liquid is in a state of metastable local equilibrium, the density fluctuations should be independent of time for time scales shorter than the characteristic relaxation time associated with the

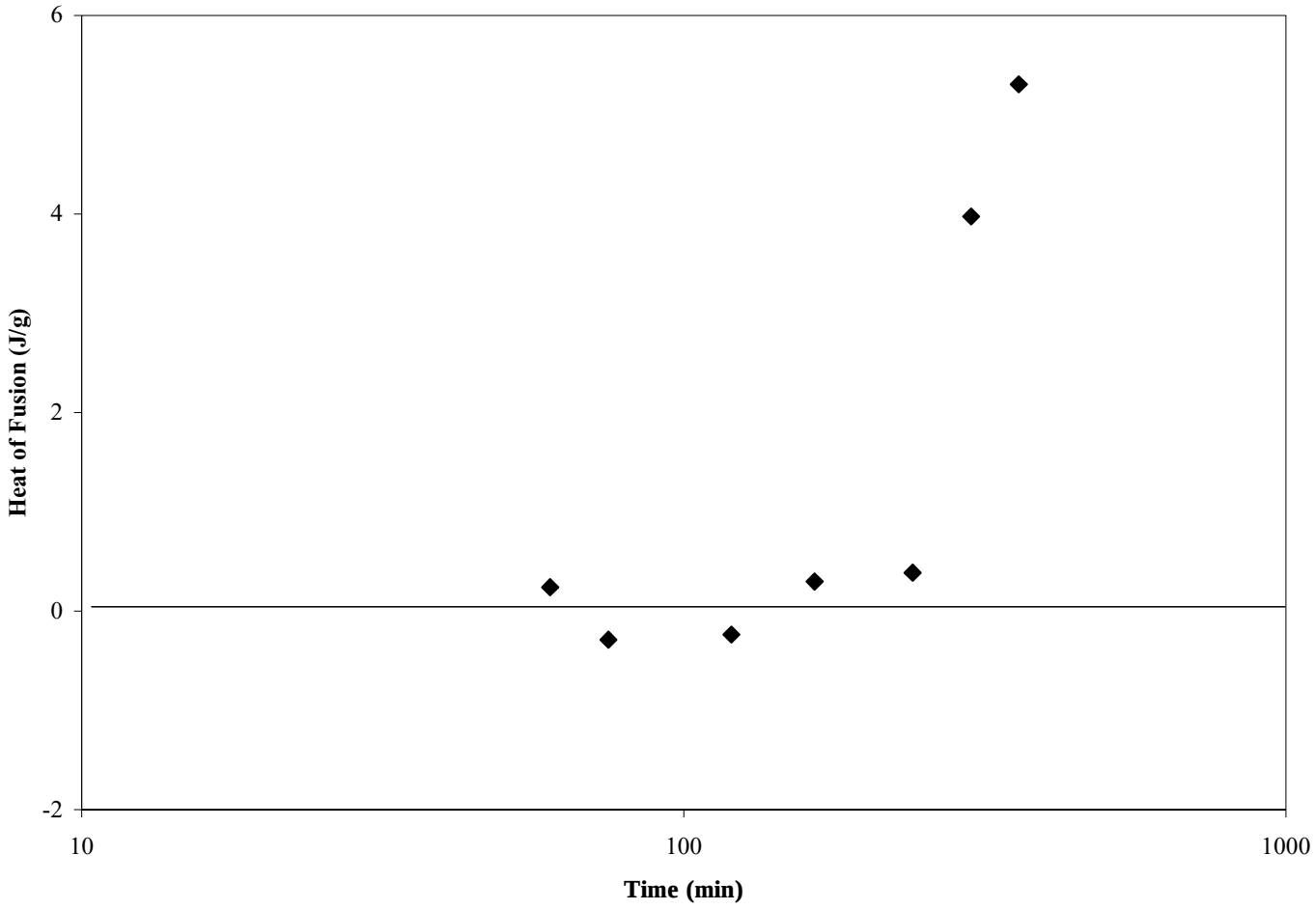

Figure 8. Evolution of the Heat of Fusion with Annealing Time for Polycarbonate Crystallized at 190°C

metastable state. In the particular case of a supercooled liquid, which can crystallize, the fluctuations should be stable (i.e. they do not change in amplitude or in periodicity). Therefore the scattering of this metastable liquid should not change until the actual formation of a stable nucleus. On the other hand, if a polymer liquid undergoes some spontaneous process such as a spinodal decomposition-like phase separation into domains with chains having different conformations, the scattering profile should be time dependent. Scattering patterns can be presented as a one-dimensional plot of scattering intensity vs. a scattering vector or as a 2-D pattern. In using a 2-D pattern (from a 2-D detector), circular integration is performed to average the intensity information at each value of the scattering vector.

All scattering data for polycarbonate samples, annealed isothermally for times within the determined induction period, were recorded on a 2-D area detector. Figure 9a shows the scattering pattern for amorphous polycarbonate, while Figure 9b is the pattern after 10 hours of annealing at 190°C. Both scattering patterns have a directional flare along the equator and meridian, which is caused by scatter of the incident beam from the beam stop. The flare is eliminated by subtraction of the pattern of an empty cell.

After correction for beam stop flare, the data were circularly averaged to determine the intensity as a function of scattering vector, q. In Figure 10, the average intensity for samples annealed for various times are plotted against the scattering vector. In looking at all scattering vectors, from 0 to 0.2 $Å^{-1}$, all eight curves show similar trends occurring through all values of q. The area of interest in these small-angle X-ray scattering patterns is below a q value of 0.04 $Å^{-1}$, and the inset of Figure 10 shows the curves (below this q value) recorded for samples annealed for different times. Even at

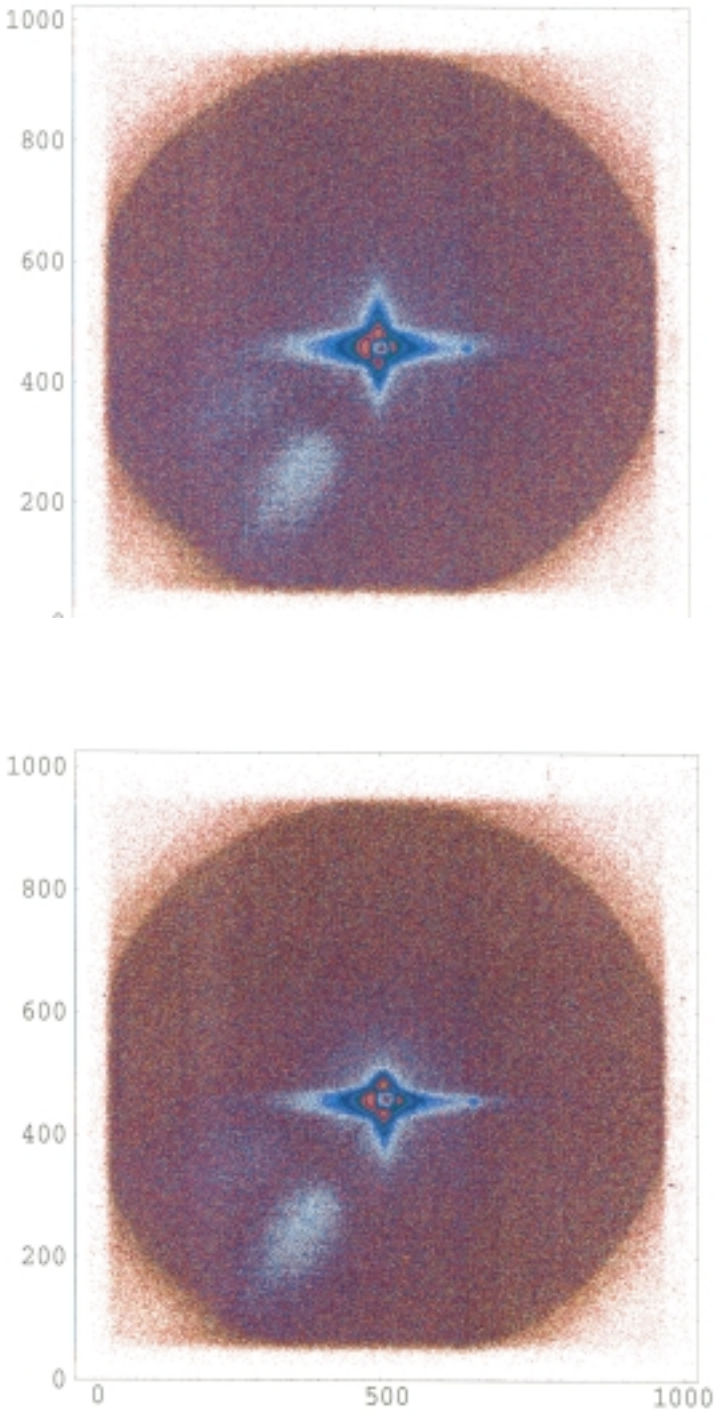

Figure 9. a) Small-Angle X-ray Scattering Pattern after 1 hour of Annealing at 190°C, and b) Small-Angle X-ray Scattering Pattern after 10 hours of Annealing at 190°C

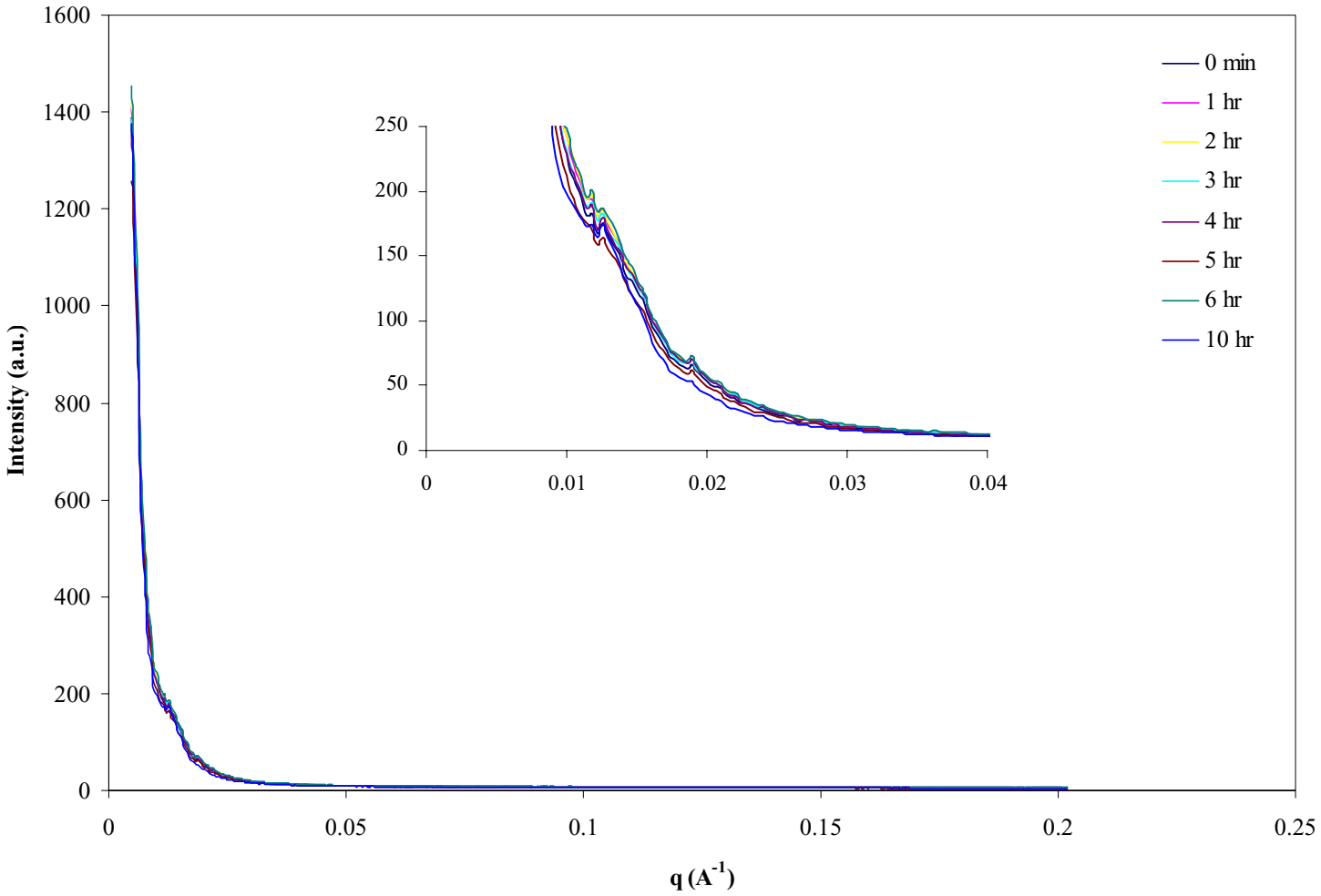

Figure 10. Plot of Small-Angle X-ray Scattering Intensity as a Function of Scattering Vector, q, for Various Annealing Times at 190°C

low angle, there is no evolution of a distinct scattering peak with increasing annealing time.

4.1.3 Wide-Angle X-ray Diffraction

Wide-angle X-ray diffraction is used principally in the structural characterization of atomic or molecular periodicity in crystalline substances. The main reason for performing wide-angle X-ray diffraction on polycarbonate samples annealed for times shorter than required for the beginning of primary crystallization, is to determine at what time crystallinity is detectable. The WAXD experiments are used for corroboration of the magnitude of the induction time determined by differential scanning calorimetry experiments. The wide-angle X-ray diffraction patterns were collected on a 2-D area detector, similar to that used to record the small-angle X-ray scattering patterns. The intensity was plotted as a function of diffraction angle, 2θ, in Figure 11. The curves in Figure 11 show some narrowing of the main peak at 18°. The peak narrows the most for annealing times ranging from 6 to10 hours, suggesting possibly that the onset of primary crystallization in bisphenol A polycarbonate at 190°C occurs after 4 or 5 hours, as suggested from the DSC studies. Data are offset along the intensity axis to make the narrowing of the peak more apparent.

4.1.4 Synchrotron Data

Wide-angle X-ray diffraction and small-angle X-ray scattering patterns were also obtained at the BNL synchrotron source to compare with these recorded on the Bruker and Metrology systems. Figure 12 is a plot of wide-angle intensity as a function of 2θ on

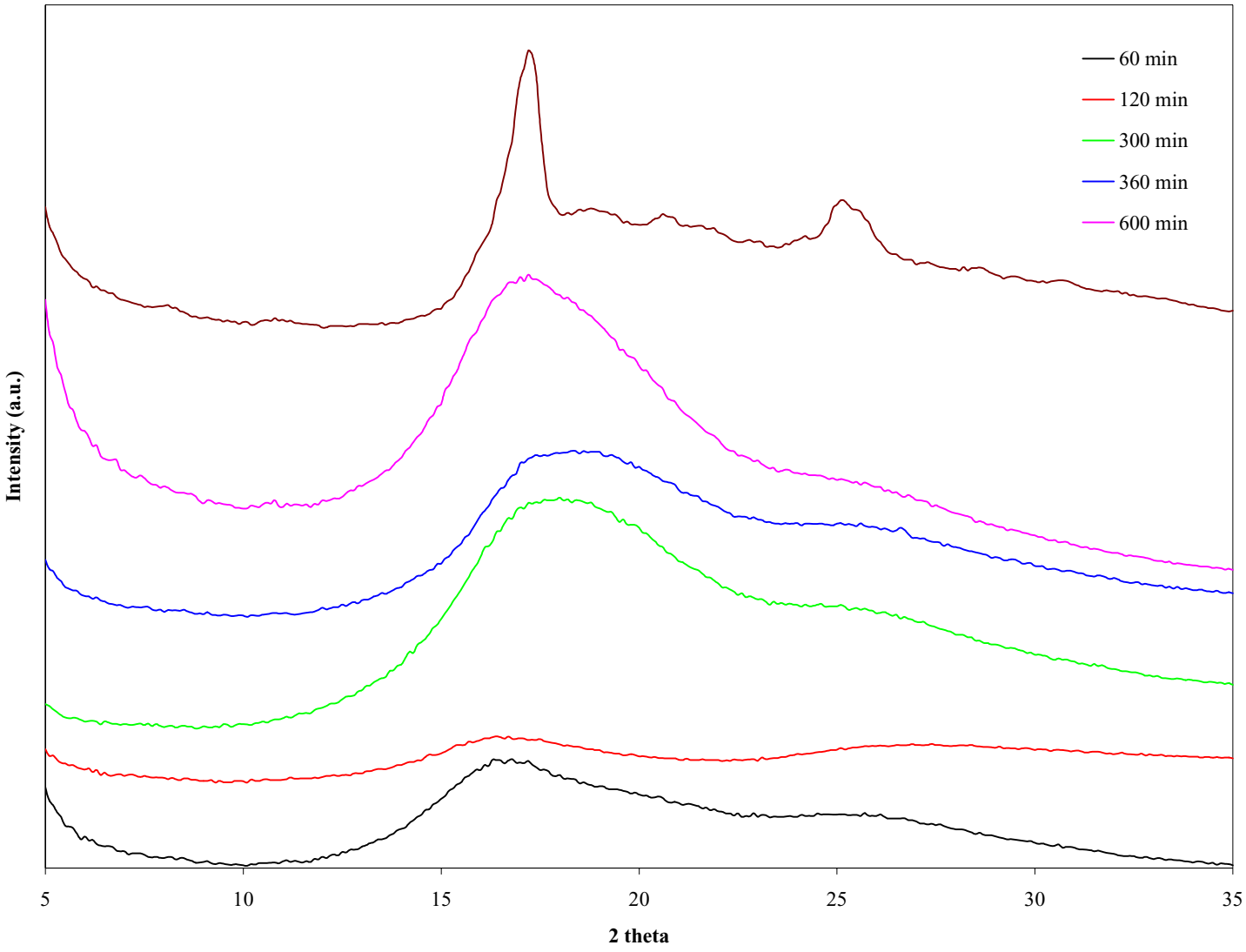

Figure 11. Wide-Angle X-ray Diffraction Pattern for Polycarbonate Annealed at 190°C for Various Times

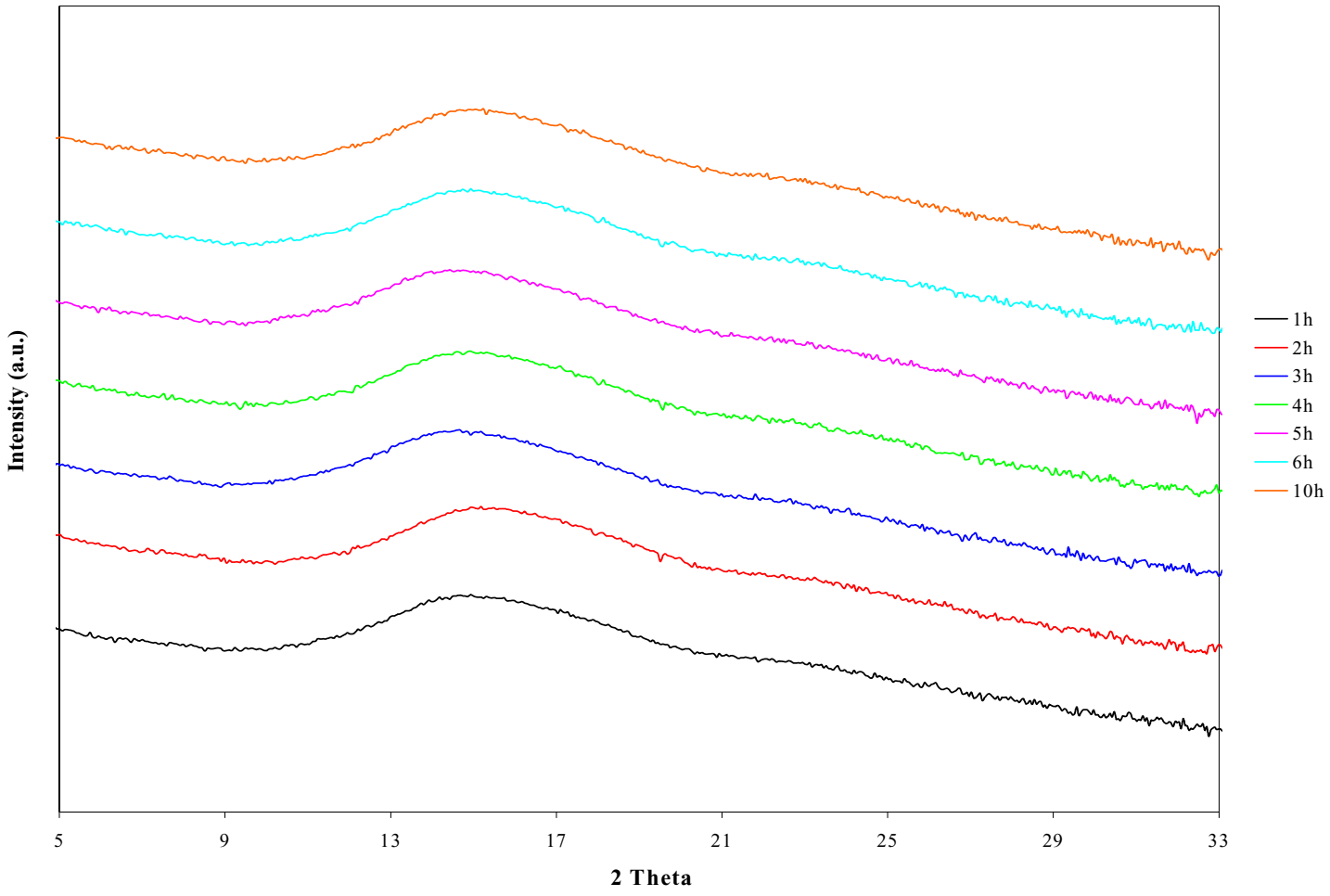

Figure 12. Wide-Angle X-ray Diffraction Pattern from Synchrotron Experiments on Polycarbonate Samples Annealed at 190°C for Various Times

an offset intensity axis. There is very little obvious difference between the curve after 1 hour of annealing at 190°C or 10 hours. Slight differences that are not detected using a line scan are seen after a detailed inspection of the 2-D wide-angle diffraction patterns. Patterns for samples annealed for 1 hour and 10 hours at 190°C are shown in Figure 13a and b, respectively. The minute differences in the patterns are seen within the inner yellow region and in the haze of the outer blue ring. In the pattern associated with the samples annealed for 10 hours, the outer ring of blue is slightly less diffuse than that observed in the patterns associated with the sample annealed for 1 hour, and the intensity increases, broadening the peaks slightly, closer to the center of the pattern (less green appears at the longer crystallization time). Because it is difficult to quantify differences in the 2-D pattern, more information may be gathered by observing the shift of the full width of the peak at the half maximum intensity. The width of the peak at the half-maximum can be calculated and plotted as a function of annealing time to determine if there is any variation in the diffraction curves. As seen in Figure 14, there is a consistent change in the peak width at half maximum as the crystallization time increases from 1 hour to 6 hours, but the data point for the sample crystallized for 10 hours does not follow the same trend. There is a possibility that the pattern recorded for the sample annealed for 10 hours is anomalous because the data point of full-width at half-maximum does not follow the same trend as the other samples, but this cannot be confirmed.

Small-angle X-ray scattering patterns for all samples, shown in Figure 15, follow the same trend and there is no evolution of the scattering profile during annealing within the induction period. There is a distinct variation in intensity that does not follow the increase of annealing time. This variation may be a result of slight orientation in the

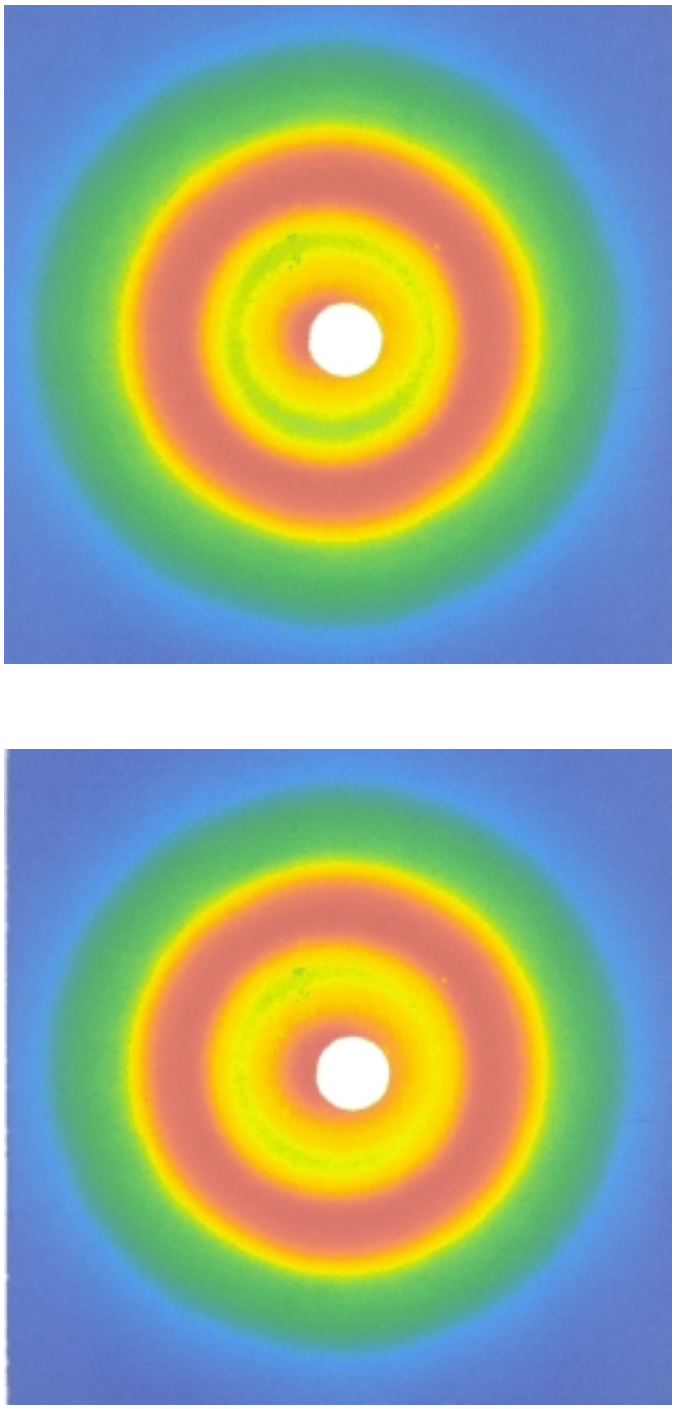

Figure 13. Synchrotron Small-Angle X-ray Scattering After a) 1 hour of Annealing at 190°C and b) 10 hours of Annealing at 190°C. The Color Intensity is the Same for Both Patterns

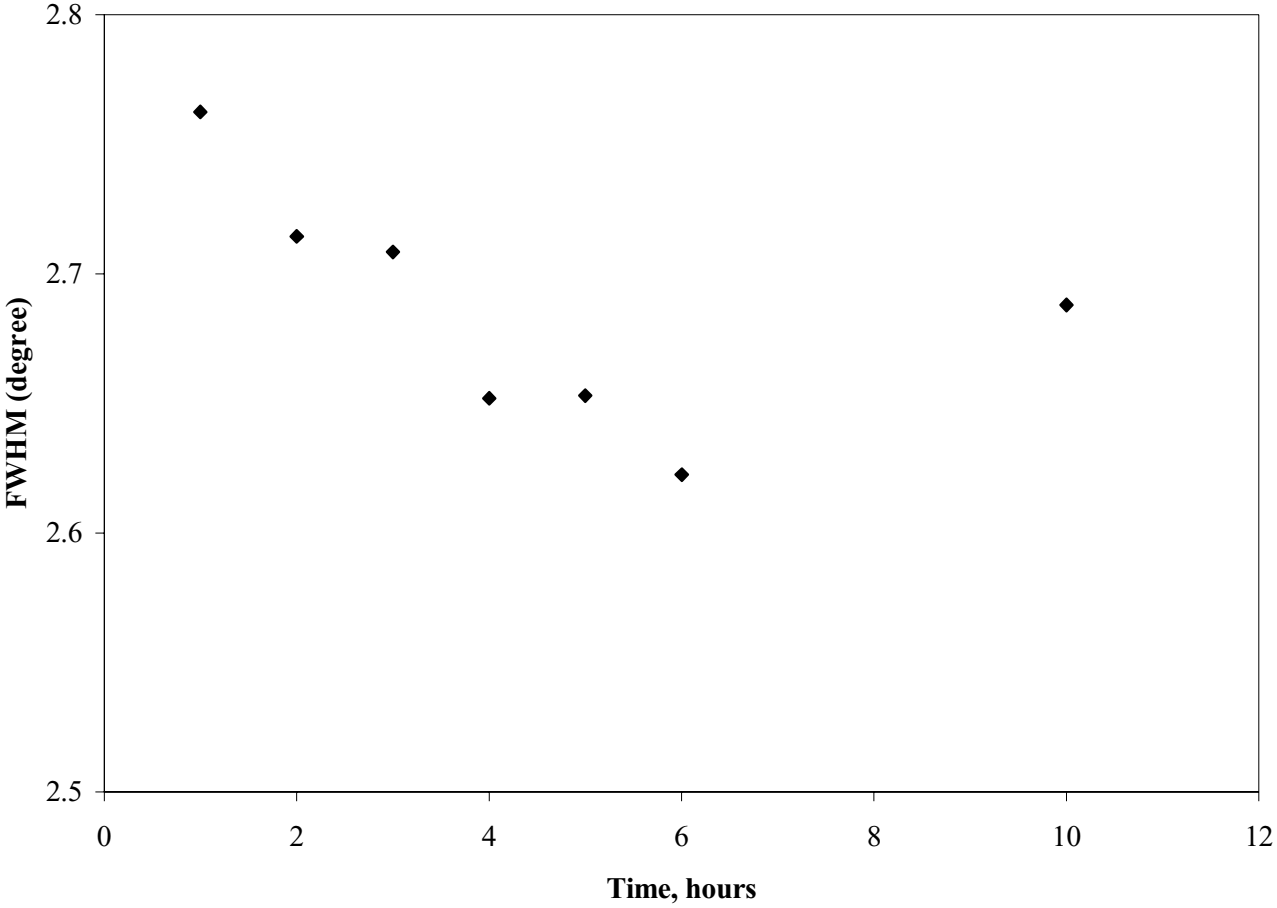

Figure 14. Plot of the Full Width at the Half Maximum of the Diffraction Peak from Synchrotron Wide-Angle X-ray Diffraction

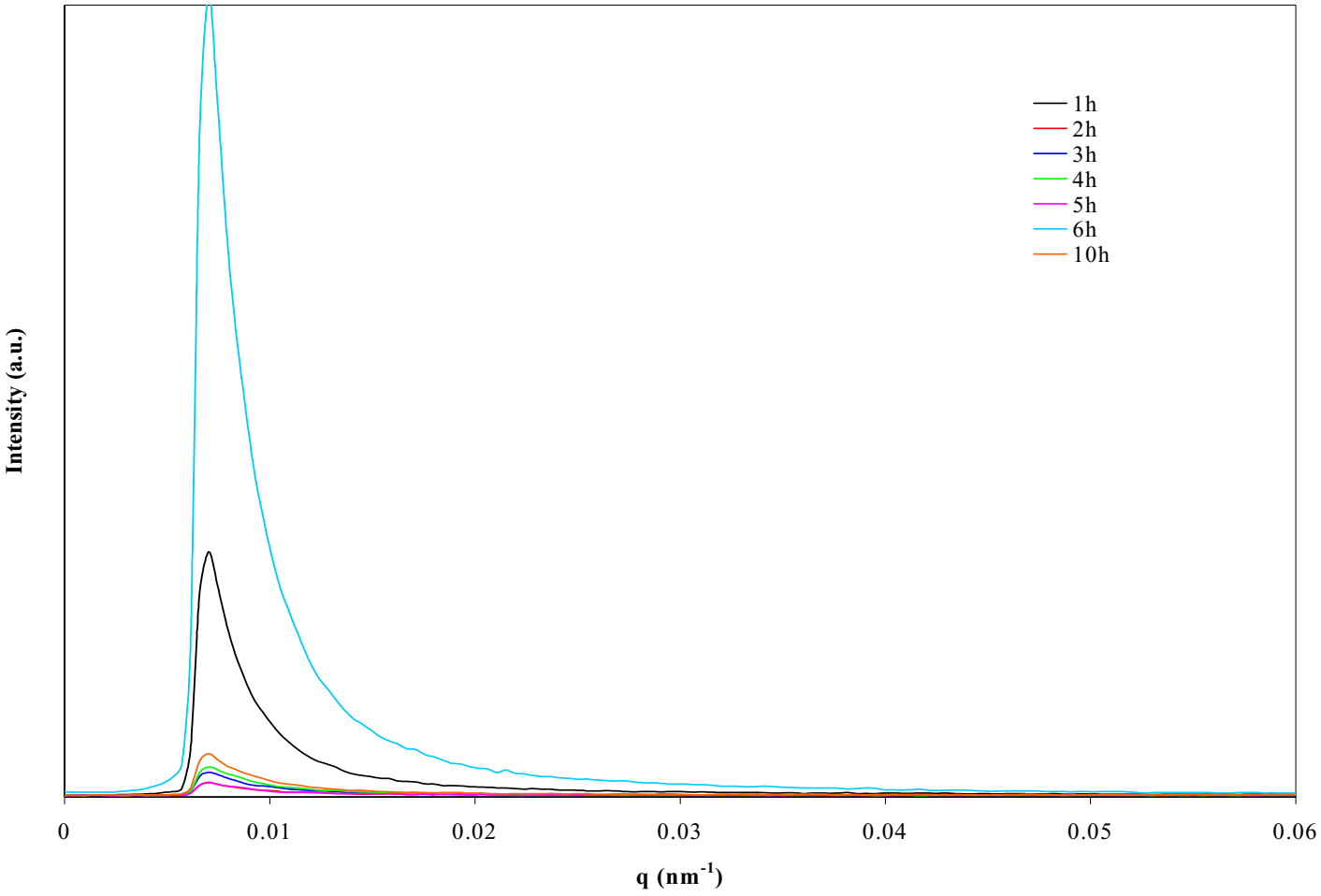

Figure 15. Small-Angle X-ray Scattering Intensity of Polycarbonate Annealed at 190°C for Various Times from Synchrotron Experiments as a Function of Scattering Vector, q

polycarbonate samples. The scattering pattern exhibits a slight anisotropy because of orientation, which invalidates the use of circular averaging; therefore line scans at arbitrary angles were taken. The low level of molecular orientation in this sample orientation is most likely the result of the melt pressing operation used in the preparation of films for SAXS analysis. While this effect was inconsequential in the other scattering experiments, it was more significant in the synchrotron SAXS experiment, since the samples were set up so the X-ray beam would hit on the edge of the sample, where more significant orientation can be caused by the flow behavior at the thinner edge of the sample. The angle at which the line scan was taken could cause the variations in intensity and peak width for the small-angle X-ray scattering data.

Overall, results from the synchrotron experiments are similar to that of the scattering and diffraction performed on other equipments. Data from these experiments are used as corroborating evidence that no crystallinity is detected in the first four to five hours of annealing.

4.1.5 Infrared Spectroscopy

As a polymer crystallizes, sections of polymer chains change conformation from those compatible with a random coil structure to that of lowest intramolecular energy and highest packing efficiency, which characterizes the chain conformation in the crystalline structure. This change in chain conformation can be quantified by infrared spectroscopy. Crystallization is observed by infrared spectroscopy when bands specific to bond vibration in a crystal environment appear in a spectrum at the expense of bands specific to bond vibration in the amorphous state. The region of interest in the spectrum of bisphenol A polycarbonate is between 1400 and 1000 cm^{-1}.

Figure 16 shows spectra with annealing times ranging from 0 minutes to 330 minutes, well beyond the expected induction period of 240 minutes. As the sample of polycarbonate is held at 190°C, the spectra shown in Figure 16 have the same shape, but shift to higher absorbance values for all wave numbers, ν, as the annealing time increases. Because there is no noticeable variation in the spectra up to 330 minutes, a spectrum of a polycarbonate sample crystallized at 190°C for four days was taken to compare to the spectra taken within the induction period. The comparison of the spectra is shown in Figure 17. The spectrum of the semicrystalline polycarbonate shows the formation of a doublet in the range of 1150 to 1250cm^{-1}, which is not seen in Figure 16 for the sample annealed for the longest time. Bands observed in the spectrum of the sample annealed for 330 minutes at wave numbers around 1120, 1285, and 1305cm^{-1} become more distinct in the crystalline sample.

4.2 Discussion

Differential scanning calorimetry studies lead to the suggestion that the induction period lasts between four and five hours. The analysis of all x-ray diffraction and infrared spectroscopy data is based on this induction period. Wide-angle x-ray diffraction was performed on the samples annealed at times that encompass the induction period. The slight narrowing observed in the diffraction peak at 18° 2θ for the sample annealed for 10 hours suggests that primary crystallization has just commenced and indicates that X-ray diffraction is less sensitive than calorimetry to detect very small amounts of crystallinity for materials like bisphenol A polycarbonate. Wide-angle X-ray diffraction data obtained at the synchrotron source also show very little variation in profile for samples annealed for times ranging form 1 hour to 10 hours. The minor changes observed in the 2-D

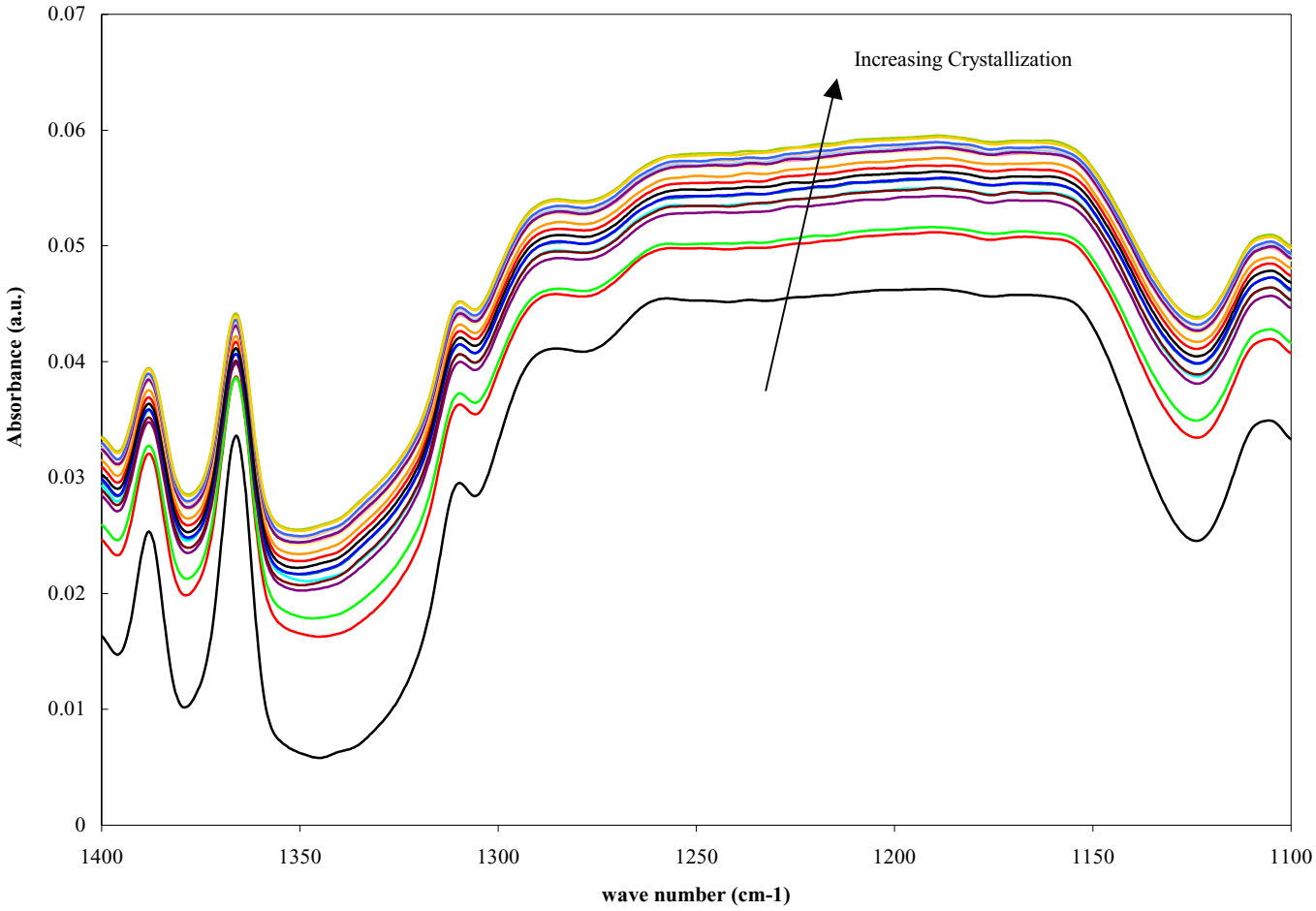

Figure 16. Infrared Spectra of Polycarbonate Measured at Various Times During Annealing at 190°C

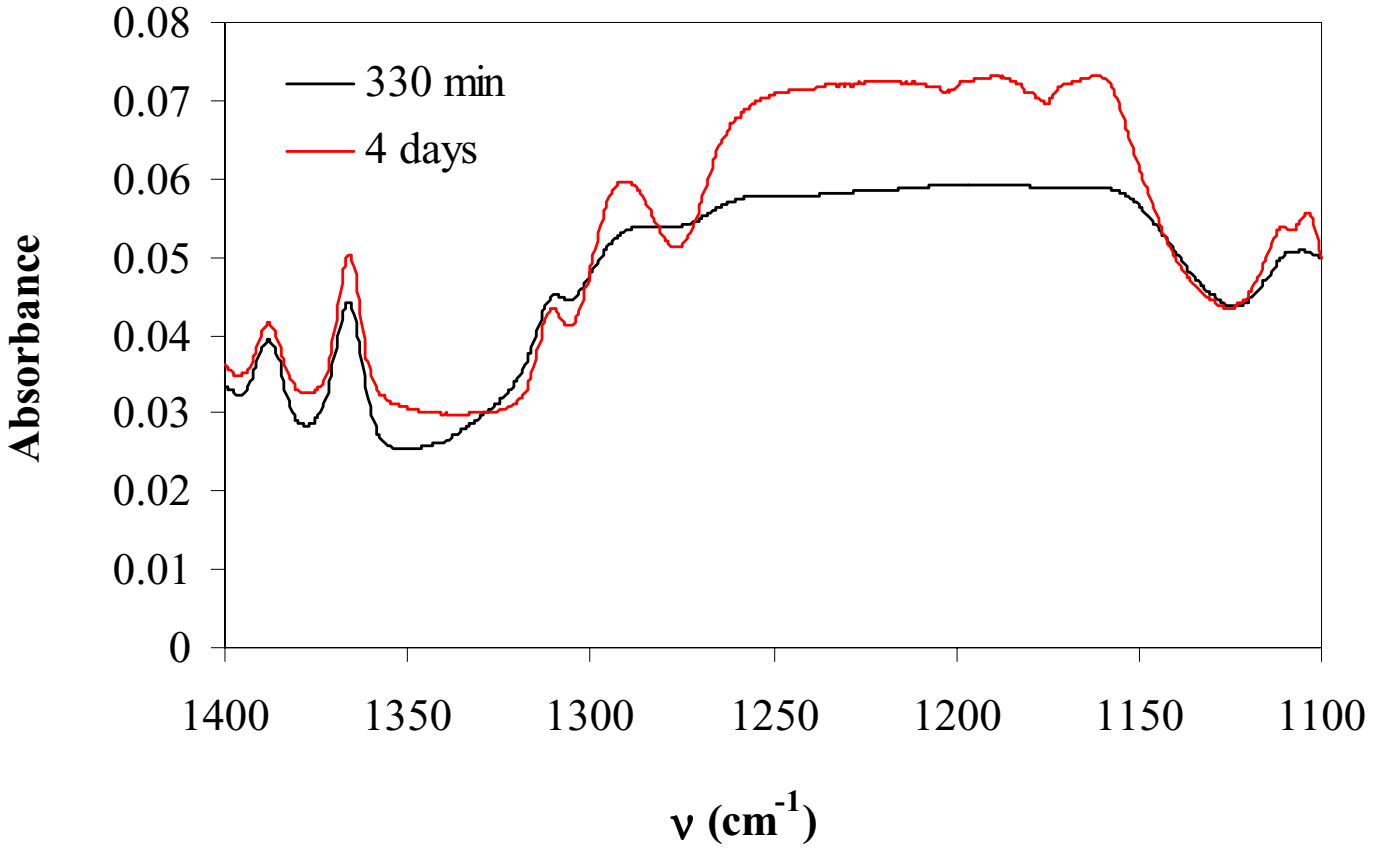

Figure 17. Comparison Between The Infrared Spectra of Polycarbonate Annealed at 190°C for 330 minutes and 4 days

diffraction pattern provide qualitative indication that there is at most a very small amount of crystallinity in the sample annealed for 10 hours. Differential scanning calorimetry can detect a minimum of about 1% crystallinity, while wide-angle X-ray diffraction is less sensitive and requires larger amount of crystallinity especially when the crystals are small. One can now focus on the analysis of small angle X-ray scattering curves for annealing times within the induction period (4 to 5 hours at 190°C).

Literature results of small angle X-ray scattering studies showed that a peak formed and shifted to lower q as the polymer was annealed within the induction period. The fact that no peak was observed to form and shift to lower q in the polycarbonate samples tested here suggests the absence of a preordering phenomenon prior to primary crystallization. Infrared spectra collected for various annealing times shift only in absorbance because as the sample is annealed at a high temperature, the polymer film thickness changes with annealing time because of creep or pressures due to sandwiching the film between KBr plates. The thickness variation cannot be quantified, but because the shape of the spectra is not change, there is no evidence of ordering during annealing. Infrared spectroscopy experiments, therefore, corroborate the SAXS conclusion since no evolution of the IR spectrum of polycarbonate was observed during the induction in the wave number range where crystalline bands are expected.

4.3 Conclusions

Although other researchers have reported an ordering process occurring prior to nucleation and growth in some polymers, the data collected in this project does not support an ordering process during the induction period for polycarbonate. Polycarbonate was studied because of the slow crystallization rate, providing a longer

period of time to study density fluctuations or conformational changes during the induction period. Using differential scanning calorimetry, the induction period for polycarbonate was determined to be four hours. Small-angle X-ray scattering studies did not show any evolution in the scattering profile with increased annealing time at 190°C. The lack of evolution of the scattering profile during the induction period leads to the conclusion that there is no preordering process occurring prior to nucleation and growth. Infrared spectroscopy confirmed that there is no spontaneous change in the population of various chain conformations during the induction period, suggesting that an ordering process is not occurring prior to nucleation and growth of crystals in 19,000g/mol polycarbonate.

Chapter 5. Isothermal Lamellar Thickening

5.1 Results

5.1.1 Differential Scanning Calorimetry

As a sample is annealed after crystallization, it is known that the melting temperature shifts to higher temperature with increased annealing time. The crystallization of polycarbonate yields two melting endotherms. When the polymer is annealed between these endotherms, the higher endotherm shifts to higher temperature and increases in area. Figure 18 is a heating trace of polycarbonate crystallized at 195.6°C, which was calculated using the Hoffman-Weeks relationship between melting temperature and crystallization temperature, for eight days then annealed at 223°C for different times. The multiple melting behavior seen in the unannealed sample is eliminated after annealing for 60 minutes. There is a shift in the melting peak to higher temperature, as expected. A plot of melting point vs. the log of annealing time is shown in the inset of Figure 18. The melting temperature of the polycarbonate samples shifts approximately 5°C over a span of 600 minutes of annealing. The relationship between log annealing time and melting temperature is nearly linear with the data exhibiting only slight deviations from a straight line.

To produce a larger shift in melting temperature with time, new samples were crystallized at 184.2°C (from Hoffman-Weeks relationship) for 8 days and annealed at 228°C for the same time durations as previously. In Figure 19, the heating traces of polycarbonate annealed at 228°C are shown to change after only 30 minutes and maintain

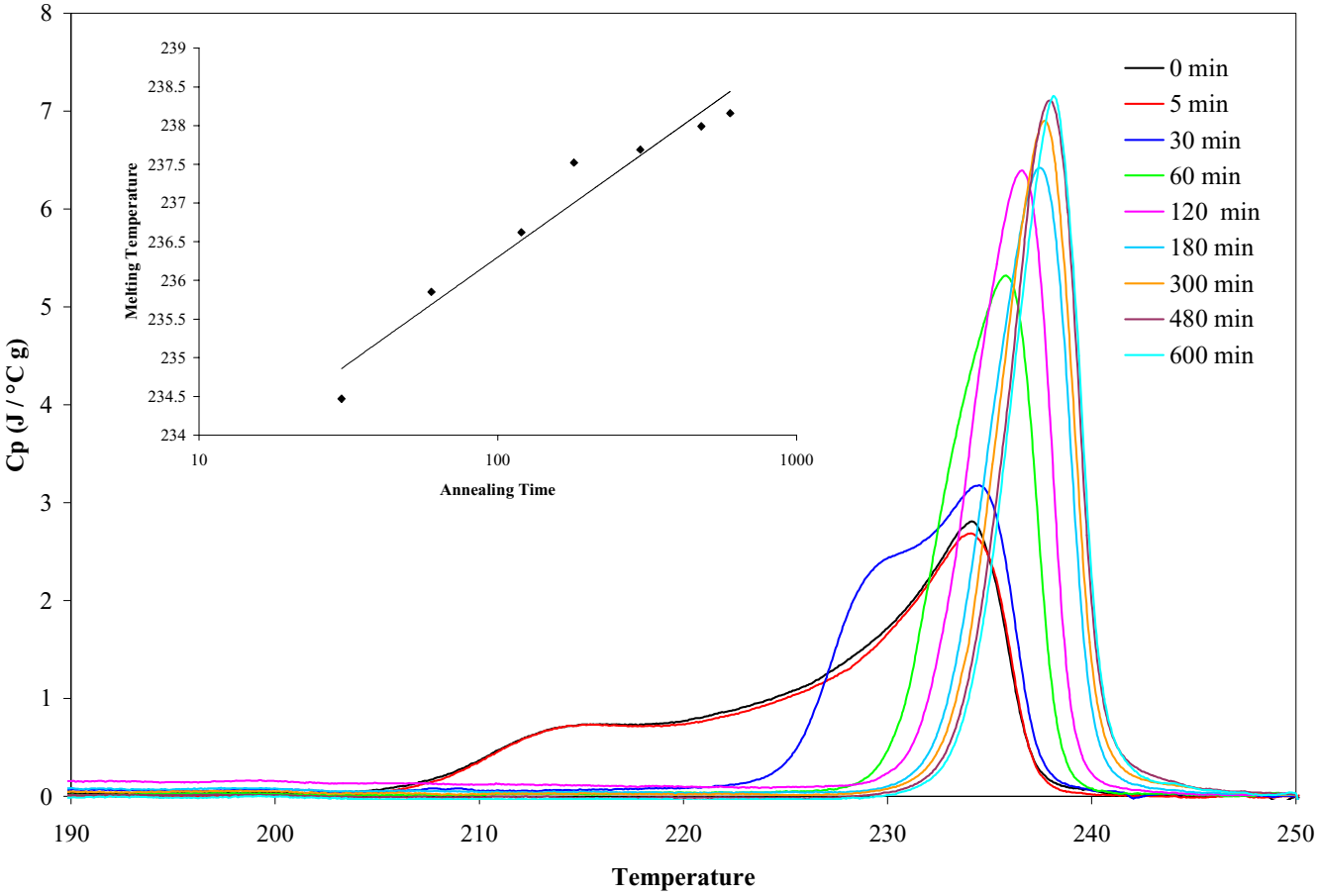

Figure 18. Heating Trace of Polycarbonate Crystallized for 8 days at 196.5°C and Annealed at 223°C for Various Times. Inset Shows the Variation of Melting Temperature with Annealing Time

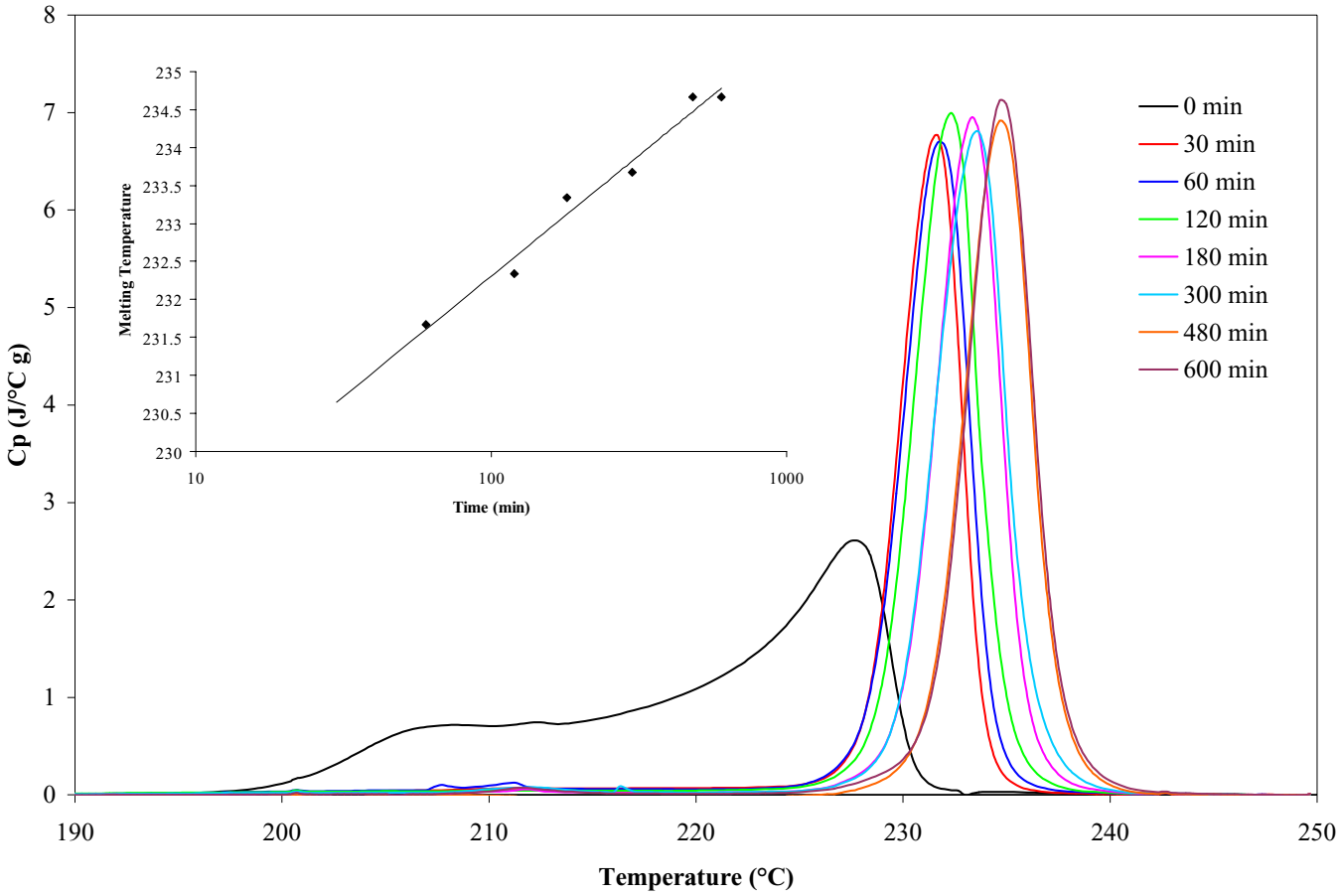

Figure 19. Heating Trace of Polycarbonate Crystallized for 8 days at 184.2°C and Annealed at 228°C for Various Times. Inset Shows the Variation of Melting Temperature with Annealing Time

the same shape for the remaining samples. There is a shift in melting temperature with annealing time, but the shift is less than that seen in samples annealed at 223°C (Figure 19 inset). Because the samples were crystallized at a lower temperature, the melting temperatures reported for samples annealed at 228°C are lower than melting temperatures reported for samples annealed at 223°C.

5.1.2 Small-Angle X-ray Diffraction

A plot of small-angle X-ray scattering intensity as a function of scattering vector for samples crystallized at 195.6°C and annealed at 223°C is shown in Figure 20. These data were calculated using the Fortran program in which masking was not taken into account. The plot in Figure 21 shows the same data from the scattering experiments analyzed with the Igor program written by Prof. Dale Schaeffer. In comparison to Figure 20, the peaks occurring at $0.035Å^{-1}$ in Figure 21 are more defined and shifted to lower q because of the masking of extraneous data. Data were recorded up to a scattering vector of $0.2Å^{-1}$, but both plots show the results only in the regions of interest. Further analysis of small-angle X-ray scattering data is carried out with scattering curves obtained through the Igor analysis using the masking process. In Figure 21, when comparing the unannealed sample to the sample annealed for 30 minutes, there is a large shift to lower q values, indicating, as expected, an increase in lamellar thickness. On the other hand, with increased annealing time, there is no systematic shift of the peak to lower q as would be expected. Figure 22 is a plot of the scattering data taken for samples annealed at 228°C and analyzed with the masking process. The scattering peak for these samples shifts to higher scattering vector values as the annealing time increases. It should be noted for both sets of samples that there is not a systematic shift in intensity with annealing time.

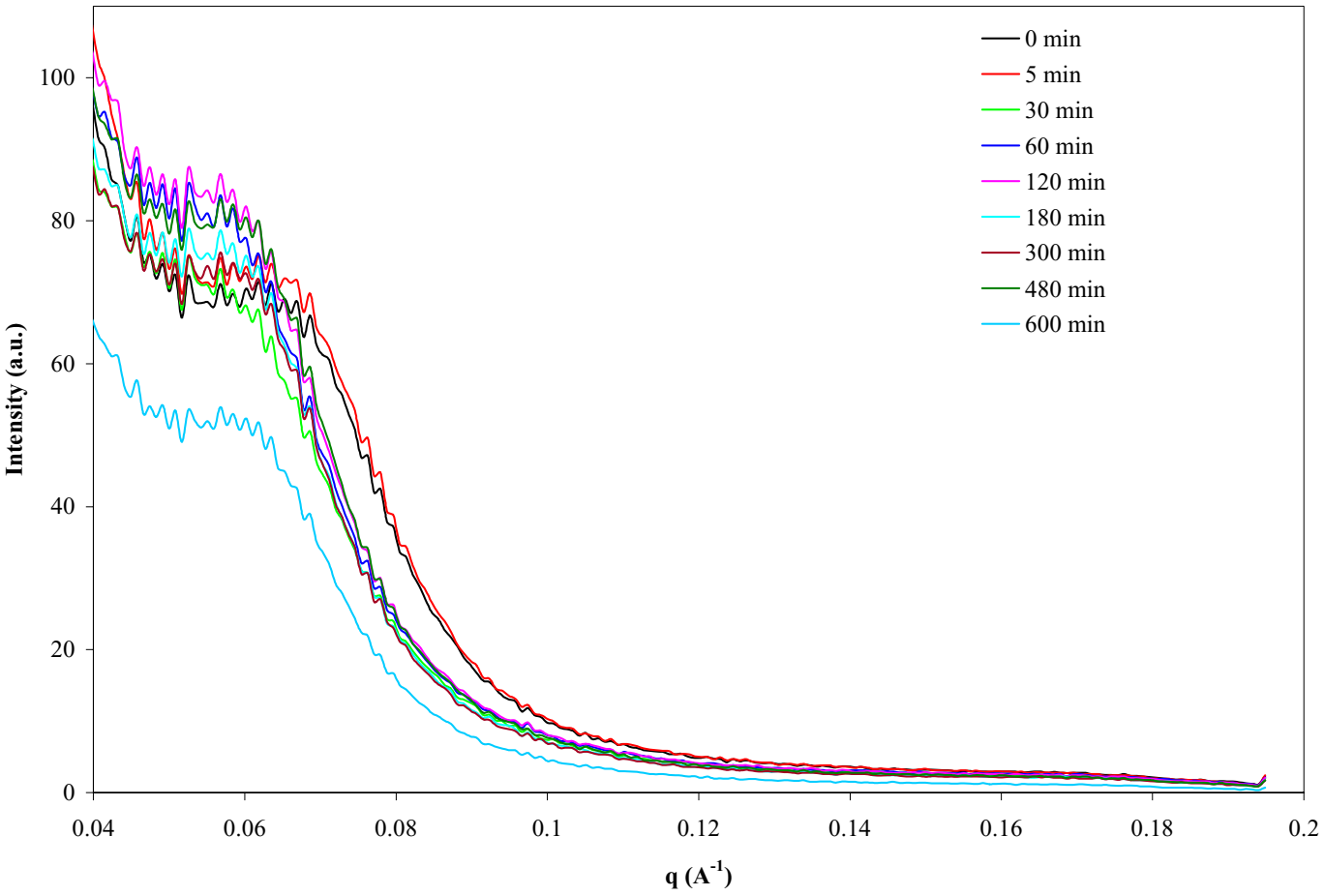

Figure 20. Small-Angle X-ray Scattering Intensity as a Function of Scattering Vector, q, for Polycarbonate Crystallized at 196.5°C for 8 Days and Annealed at 223°C for Various Times. Integration by Fortran Program

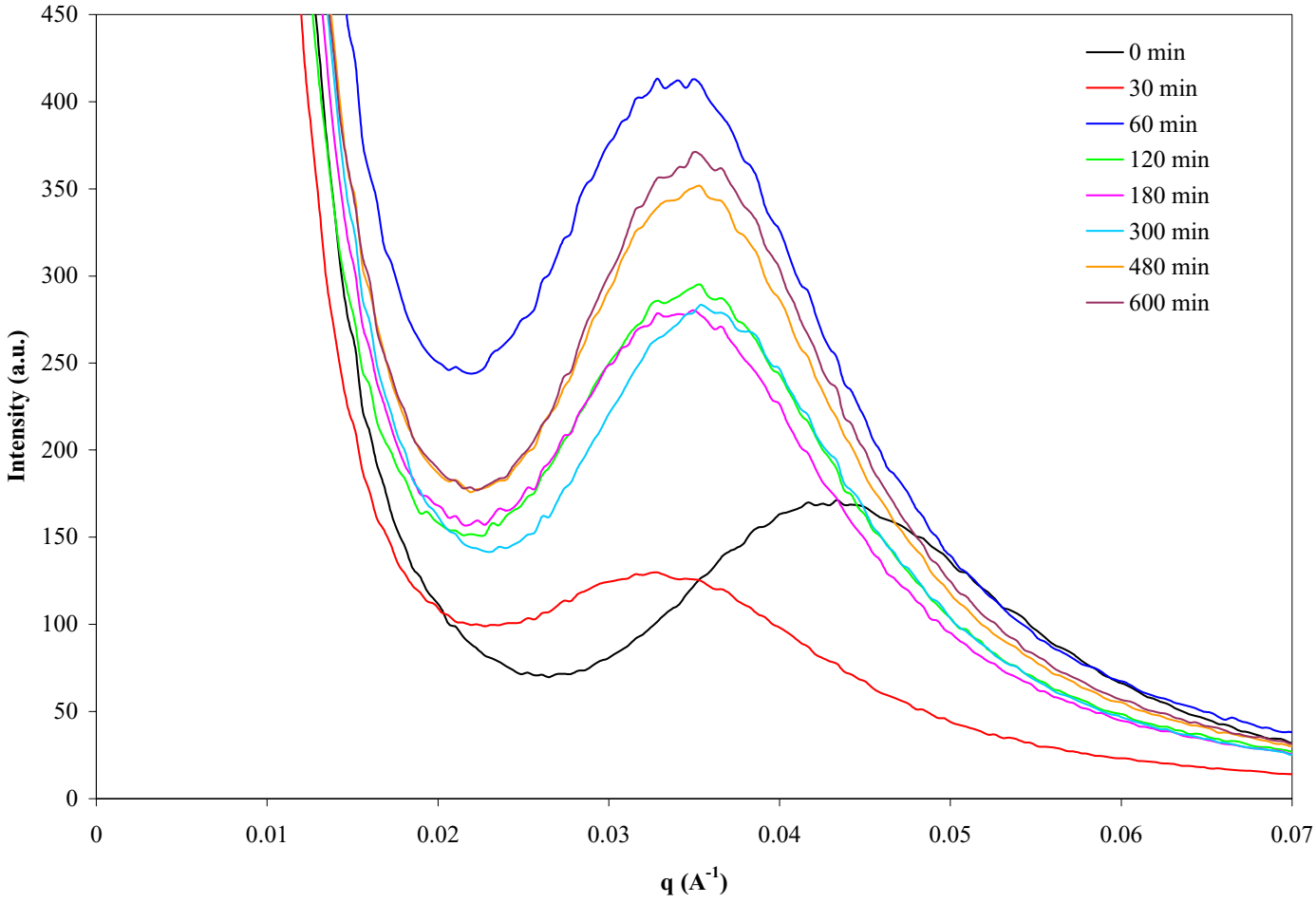

Figure 21. Small-Angle X-ray Scattering Intensity as a Function of Scattering Vector, q, for Polycarbonate Crystallized at 196.5°C for 8 Days and Annealed at 223°C for Various Times. Integration by Igor Subroutine

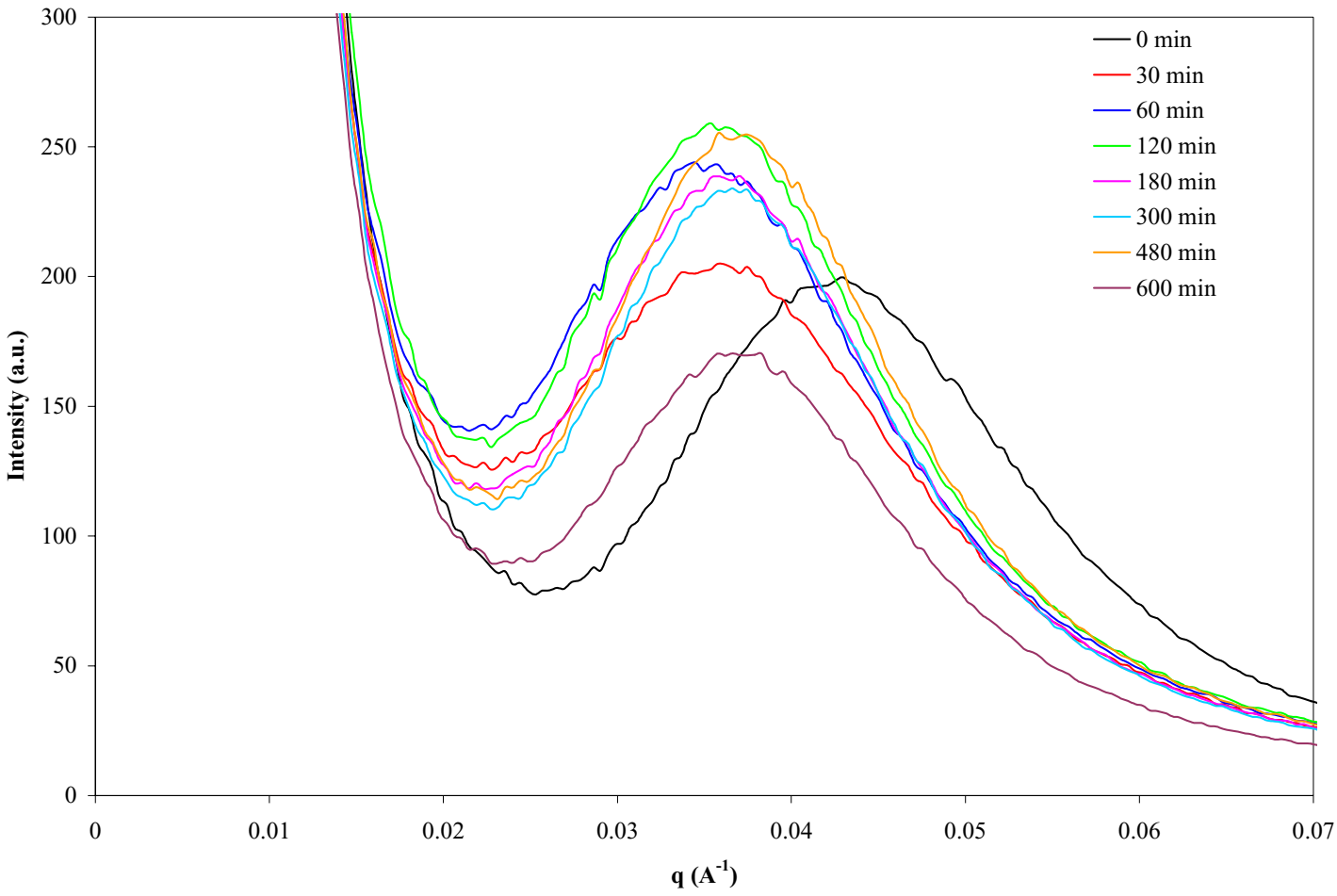

Figure 22. Small-Angle X-ray Scattering Intensity as a Function of Scattering Vector, q, for Polycarbonate Crystallized at 184.2°C for 8 Days and Annealed at 228°C for Various Times. Integration by Igor Subroutine

The magnitude of the scattering vector at the maximum of the scattering peak is obtained after Lorenz correction. A Lorenz corrected scattering curve is shown in Figure 23. A well-defined peak is shown when the intensity is multiplied by the square of the scattering vector and plotted as a function of scattering vector. This peak position is inversely proportional to the long spacing (combined crystalline and amorphous layer thickness). Further analysis yields the lamellar thickness of the polycarbonate sample. The long spacing and the lamellar thickness are related by the crystallinity of the sample. Crystallinity was determined using the ratio of the heat of fusion found using DSC and the theoretical heat of fusion, which was taken as 130J/g. Tables 1 and 2 are a compilation of long spacing and crystallinity for both annealing temperatures. The long spacing values are around 150Å to 165Å for samples that were annealed, and crystallinity ranges from 20 to 35%. Using the Gibbs-Thomson relationship, the melting temperature can then be plotted as a function of the inverse lamellar thickness. Figure 24 is the Gibbs-Thomson plot for the data measured for each set of samples. The triangles are data points from other research by Jonza et al. and Sohn et al.[16,17] The error bars are used in this plot to account for the uncertainty in lamellar thickness determined by small-angle X-ray scattering, which is assumed to be approximately ± 5 A for each data point. Using the best-fit line, the equilibrium melting temperature was calculated to be 576.07K (303°C), and the surface energy was determined to be 36.6 mJ/m^2. The values determined by Sohn and Jonza for the equilibrium melting temperature were 324°C and 335°C, and the surface free energies are 70 and 52 mJ/m^2, respectively.[16,17]

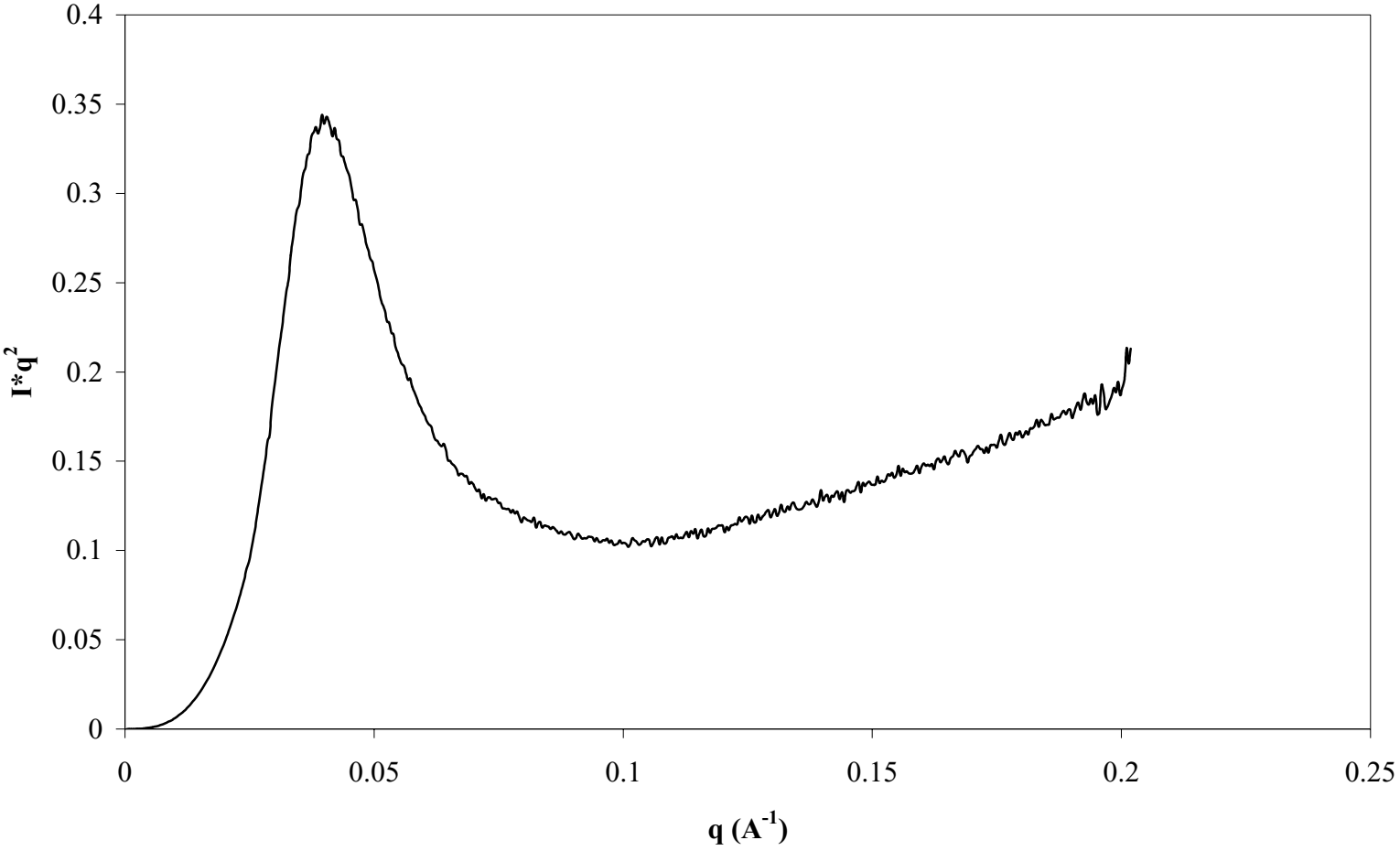

Figure 23. Sample Lorenz Correction Curve

T_a = 223°C	Long Spacing (Å)	Crystallinity (%)	Lamellar Thickness (Å)
0 minutes	132	29.0	38.3
30 minutes	154	25.1	38.7
60 minutes	159	24.2	38.5
120 minutes	159	33.9	53.9
180 minutes	155	29.0	45.1
300 minutes	155	27.5	42.8
480 minutes	155	25.2	39.2
600 minutes	154	22.9	35.3

Table 1. Compiled Data of Long Spacing and Crystallinity for Samples Annealed at 223°C for Various Times

T_a = 228°C	Long Spacing (Å)	Crystallinity (%)	Lamellar Thickness (Å)
0 minutes	130	24.5	31.8
30 minutes	170	20.0	33.9
60 minutes	164	21.7	35.7
120 minutes	164	22.2	36.5
180 minutes	162	21.8	35.3
300 minutes	162	23.3	37.8
480 minutes	162	21.3	34.6
600 minutes	162	22.9	37.2

Table 2. Compiled Data of Long Spacing and Crystallinity for Samples Annealed at 228°C for Various Times

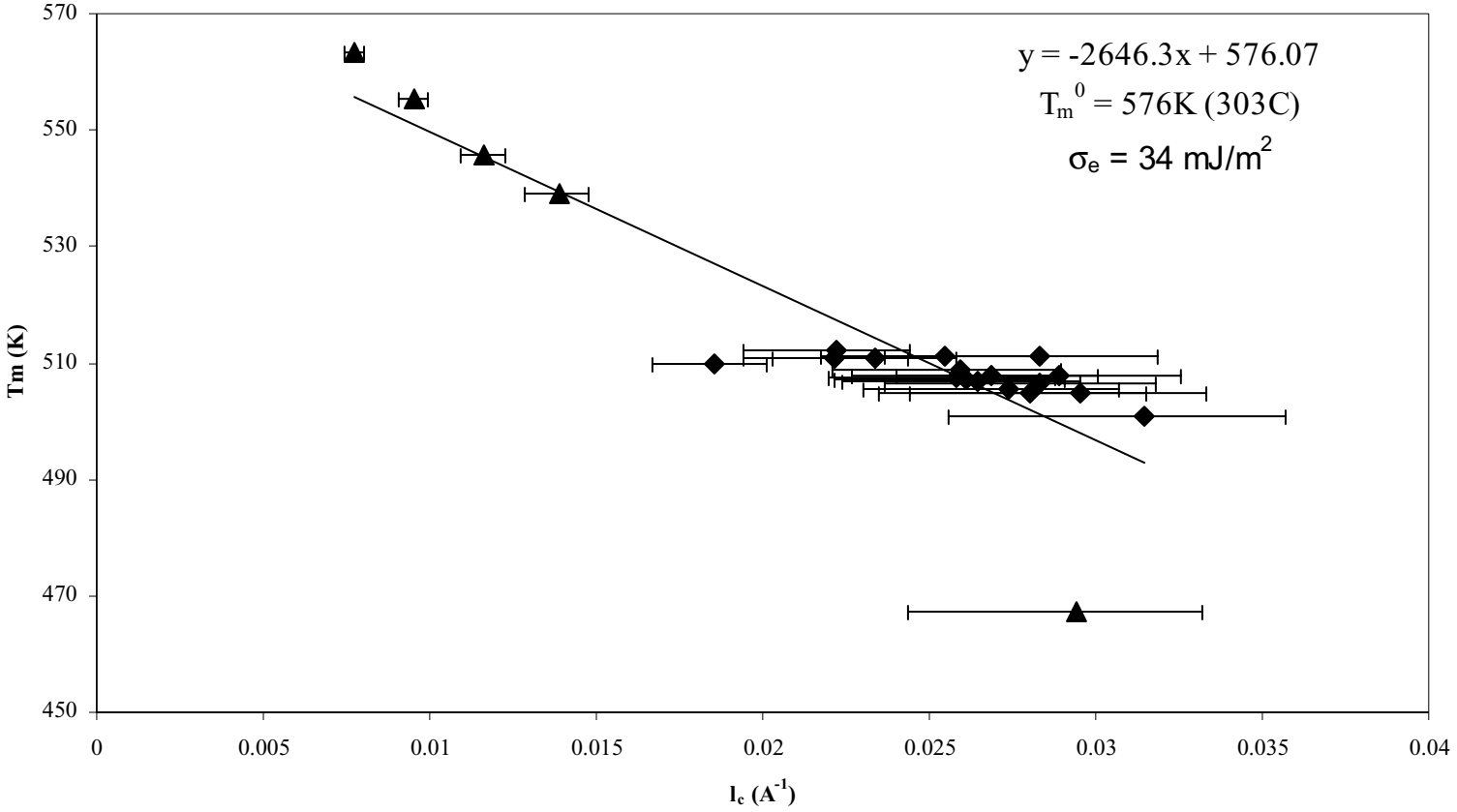

Figure 24. Gibbs-Thomson Plot of Melting Temperature as a Function of the Inverse of the Lamellar Thickness. Triangles Represent Values Reported in Literature

5.1.3 Microscopy

Samples that were microtomed were imaged under the AFM. Figures 25a and b are the images of the bulk polycarbonate samples after crystallization and annealing for 8 hours at 223°C and 228°C, respectively. The images do not convey the lamellar morphology expected for a semicrystalline polymer because the structure is smeared when the sample is cut; therefore, the thickness of the polycarbonate lamellae after annealing could not be determined by AFM. To determine an avenue for further research, some of the microtomed samples were etched using one of two solvents, but because the optimum concentration of etchant and etching time were unknown, only two samples were etched and imaged to investigate if the lamellar morphology can be observed using this sample preparation procedure. Figure 26 is a SEM micrograph of the surface morphology of a sample annealed for 5 hours at 223°C and subsequently etched with triethylamine for 5 minutes. Very little morphology is seen after this etching procedure. No morphology could be characterized as lamellae and measured for thickness. The image in Figure 27 is the sample annealed at 223°C for eight hours then etched with diethyltriamine for one minute. The structure after etching for only one minute is very open, but again, lamellar structures could not be identified with certainty, consequently, their thickness could not be measured for comparison with these obtained by small-angle X-ray scattering.

5.1.4 Epitaxial Growth

In an attempt to compare the morphology of bulk polycarbonate with that of a thin film, polycarbonate was solution cast onto p-terphenyl and calcite or spin coated onto

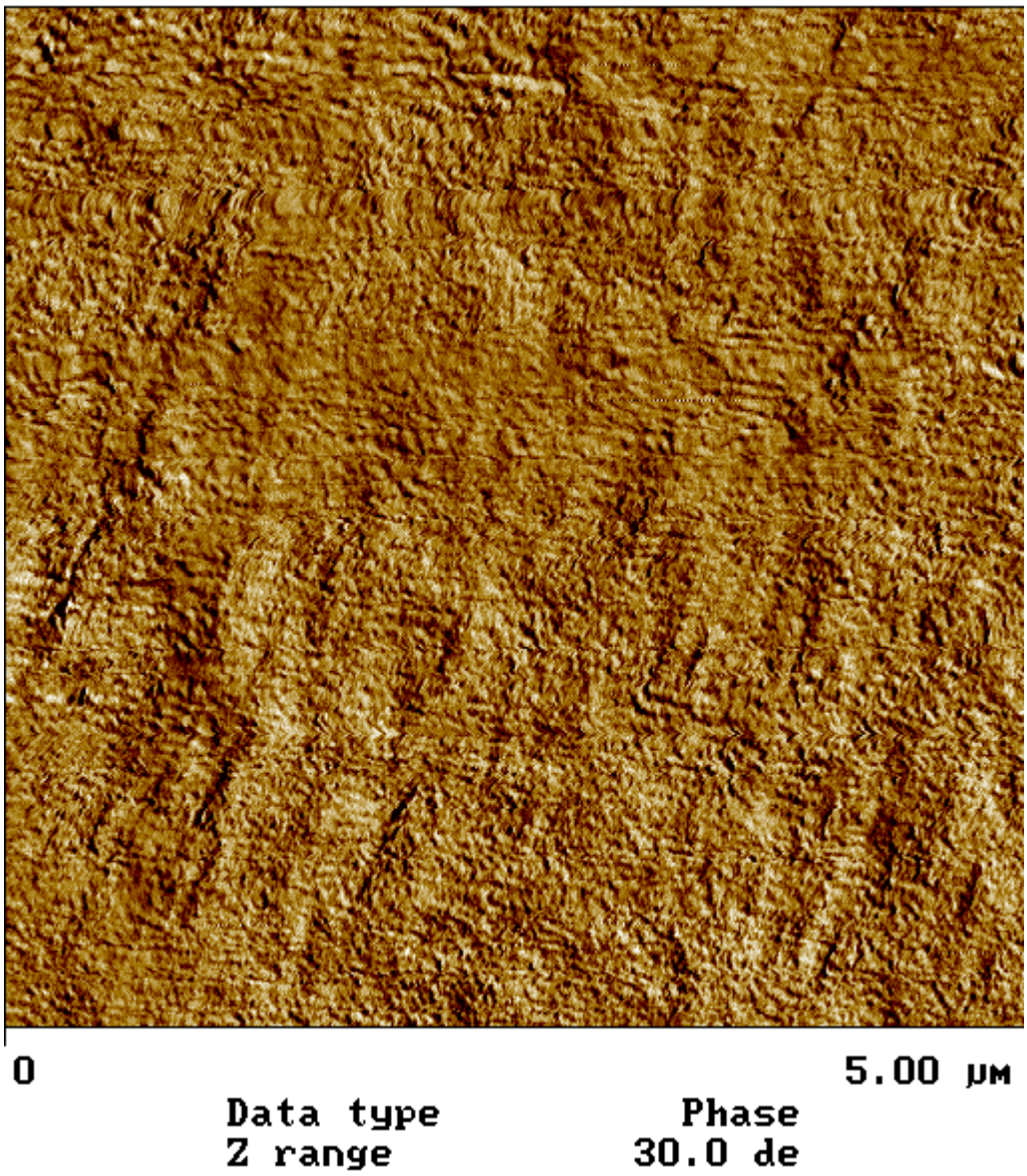

Figure 25a. Atomic Force Microscope Image of Microtomed Polycarbonate after 8 Days of Crystallization at 195.6°C and Annealing at 223°C for 8 Hours

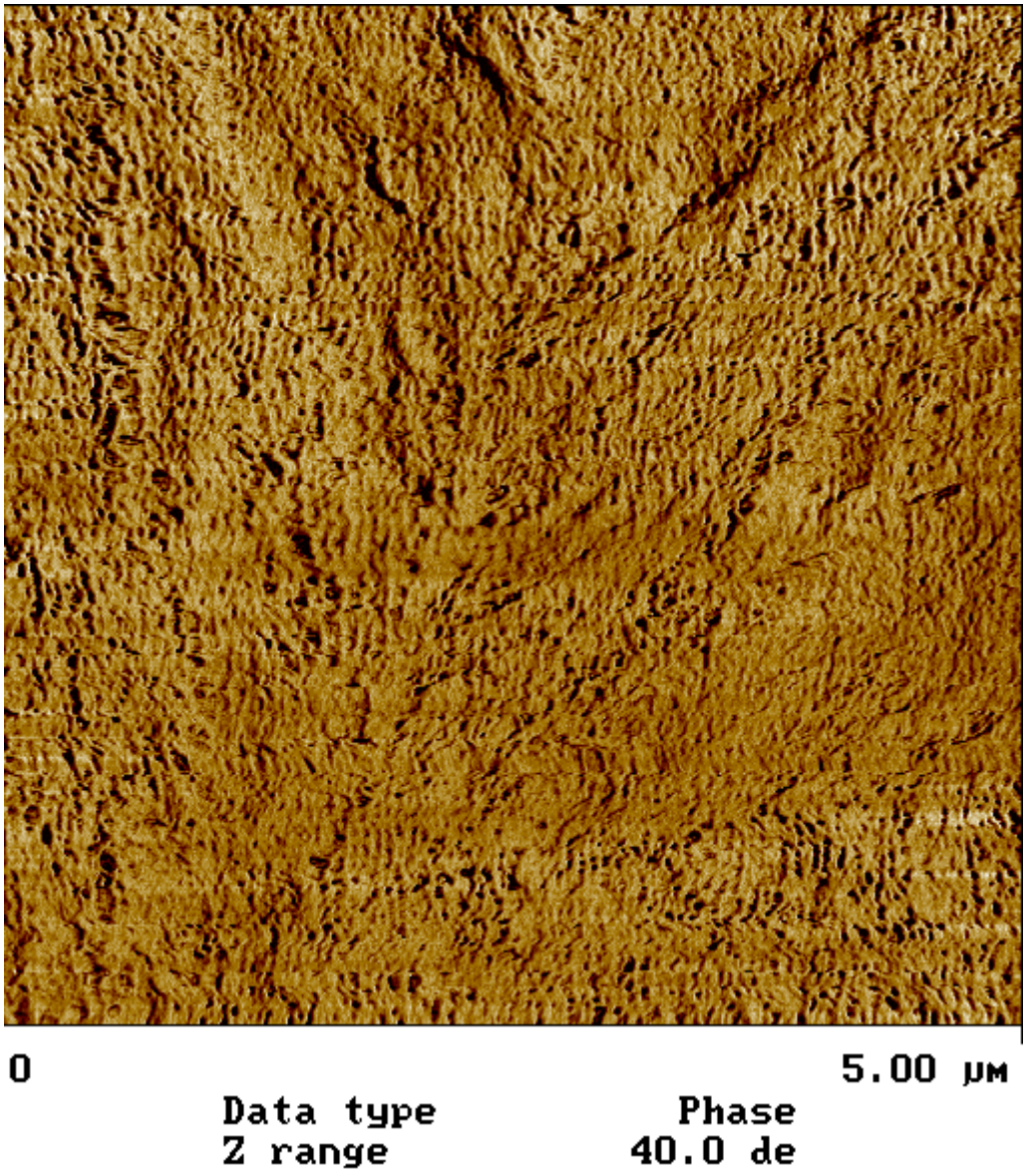

Figure 25b. Atomic Force Microscope Image of Microtomed Polycarbonate after 8 Days of Crystallization at 184.2°C and Annealing at 228°C for 8 Hours

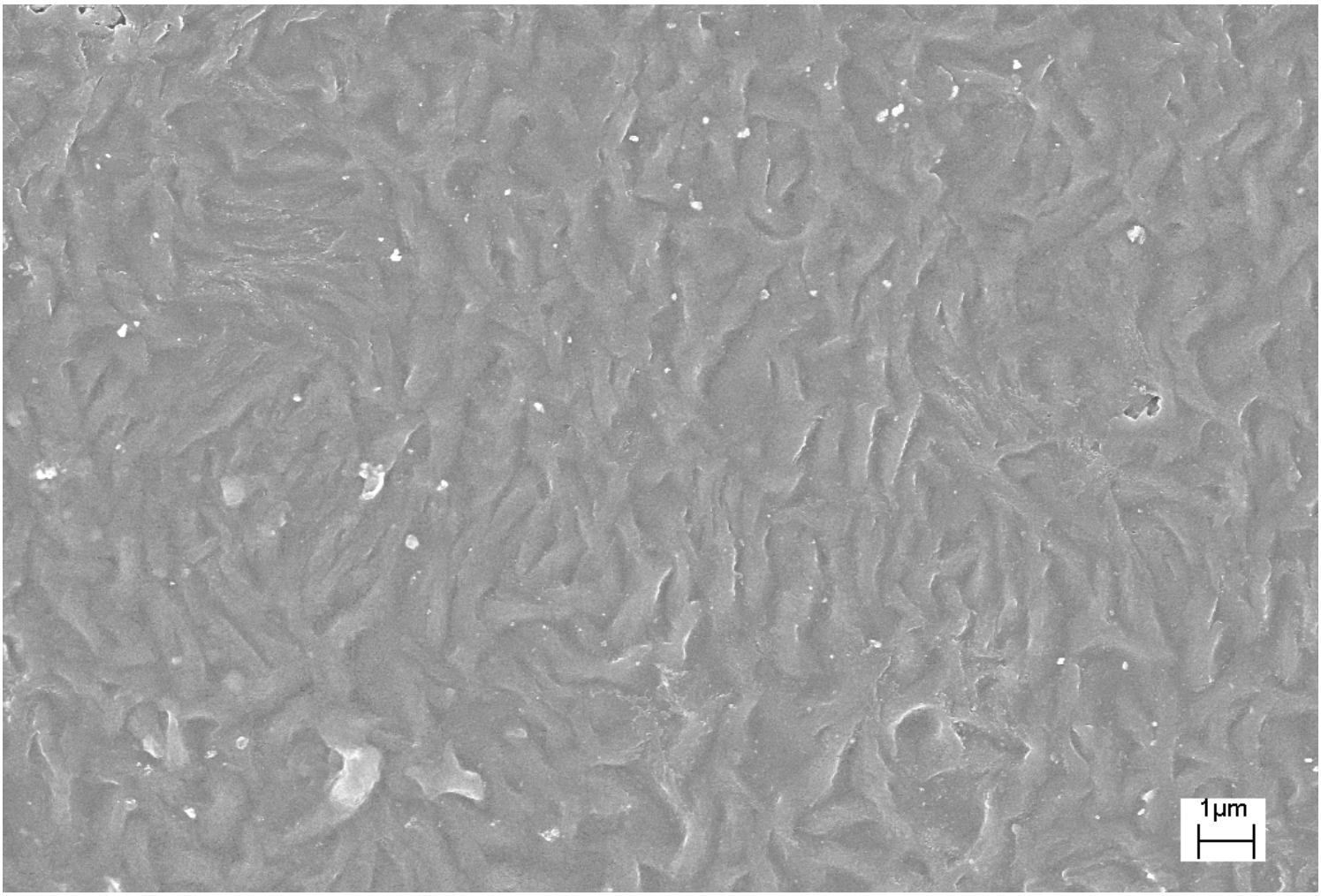

Figure 26. Polycarbonate Etched in Triethylamine for 5 Minutes After Crystallizing at 195.6°C for 8 Days and Annealing at 223°C for 5 Hours

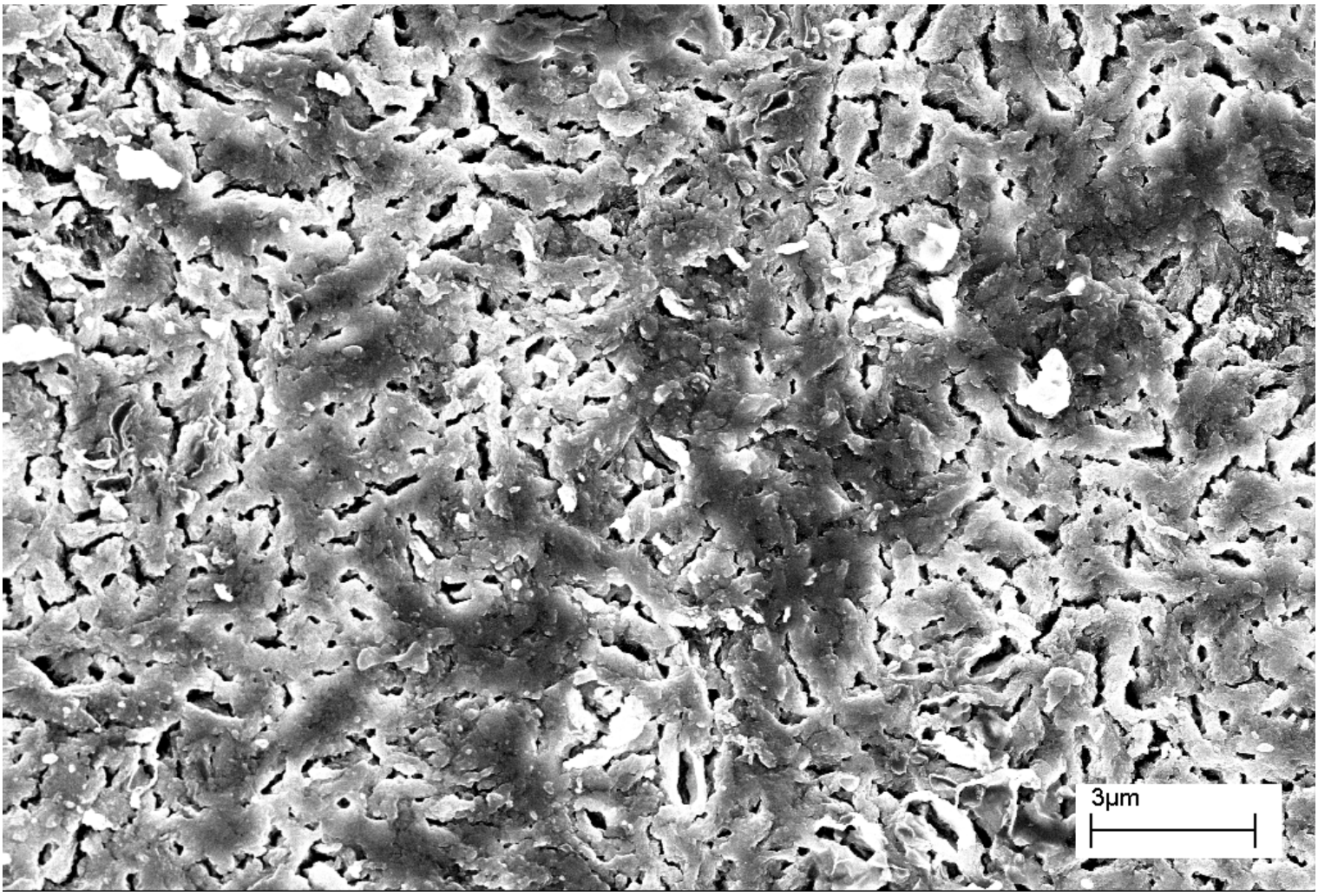

Figure 27. Polycarbonate Etched in Diethyltriamine for 1 Minute After Crystallizing at 195.6°C for 8 Days and Annealing at 223°C for 8 Hours

silicon surfaces. The samples spin coated on silicon did not show any signs of crystallization after 5 days at 190°C, so use of this substrate was abandoned. Polycarbonate crystals were shown to grow epitaxially on a p-terphenyl substrate,[22] but p-terphenyl substrates were not sufficiently stable for use under long isothermal crystallization condition. Epitaxial crystallization experiments described in the literature with p-terphenyl as a substrate were carried out with extremely low molar mass polycarbonate, which could crystallize upon cooling from the melt state. The organic p-terphenyl substrate was not sufficiently stable for crystallization under isothermal condition as it sublimes when held at 190°C for long periods of time.

Because calcite was shown to force the partial epitaxy of polycarbonate, further experiments were performed using calcite as the substrate.[17] The solution cast samples were imaged using scanning electron microscopy. The crystallization of polycarbonate was best demonstrated by using a 5 wt/wt% solution of polycarbonate and chloroform. Figure 28 shows the lamellar structure of polycarbonate after crystallization for 5 days. The voids are due to lack of polymer coverage, but lamellae, nearly perpendicular to the substrate, are clearly visible. Taking nine measurements from the same sample, the average long spacing of the polycarbonate was determined to be 151 Å.

Epitaxial growth does not rigorously occur when crystallizing polycarbonate on calcite. In Figure 29, polycarbonate crystallized on calcite for 7 days displays terrace stacking of lamellae, indicating the polymer lamellae are parallel to the substrate. The presence of a spherulitic structure is also indicative of non-epitaxial growth because the lamellae splay and branch as they radiated out from the nucleus, as shown in Figure 30. No other method of growing end-on lamellae epitaxially on the calcite surfaces was

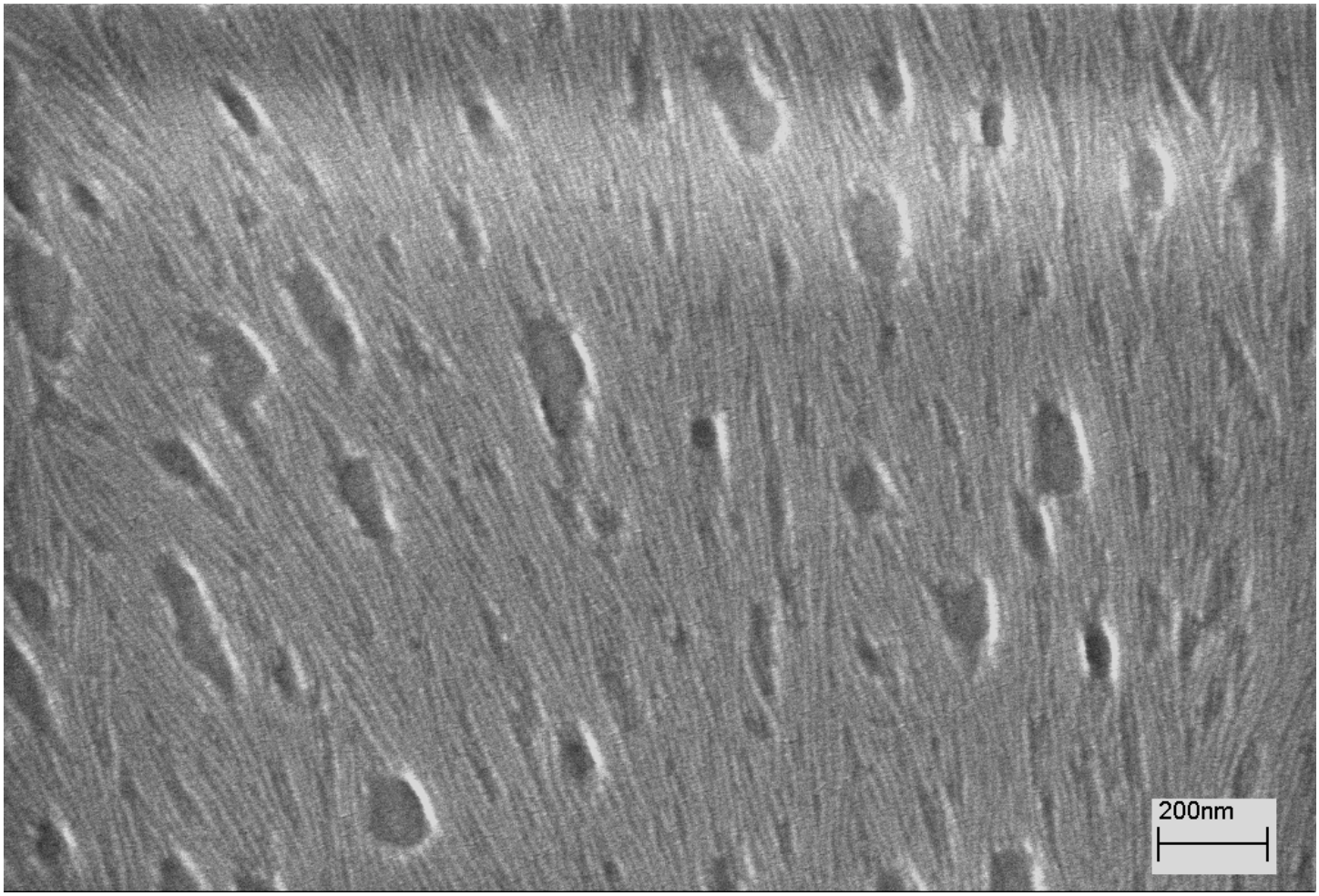

Figure 28. Scanning Electron Micrograph of 5wt% Polycarbonate in Chloroform Solution Crystallized at 190°C for 5 Days

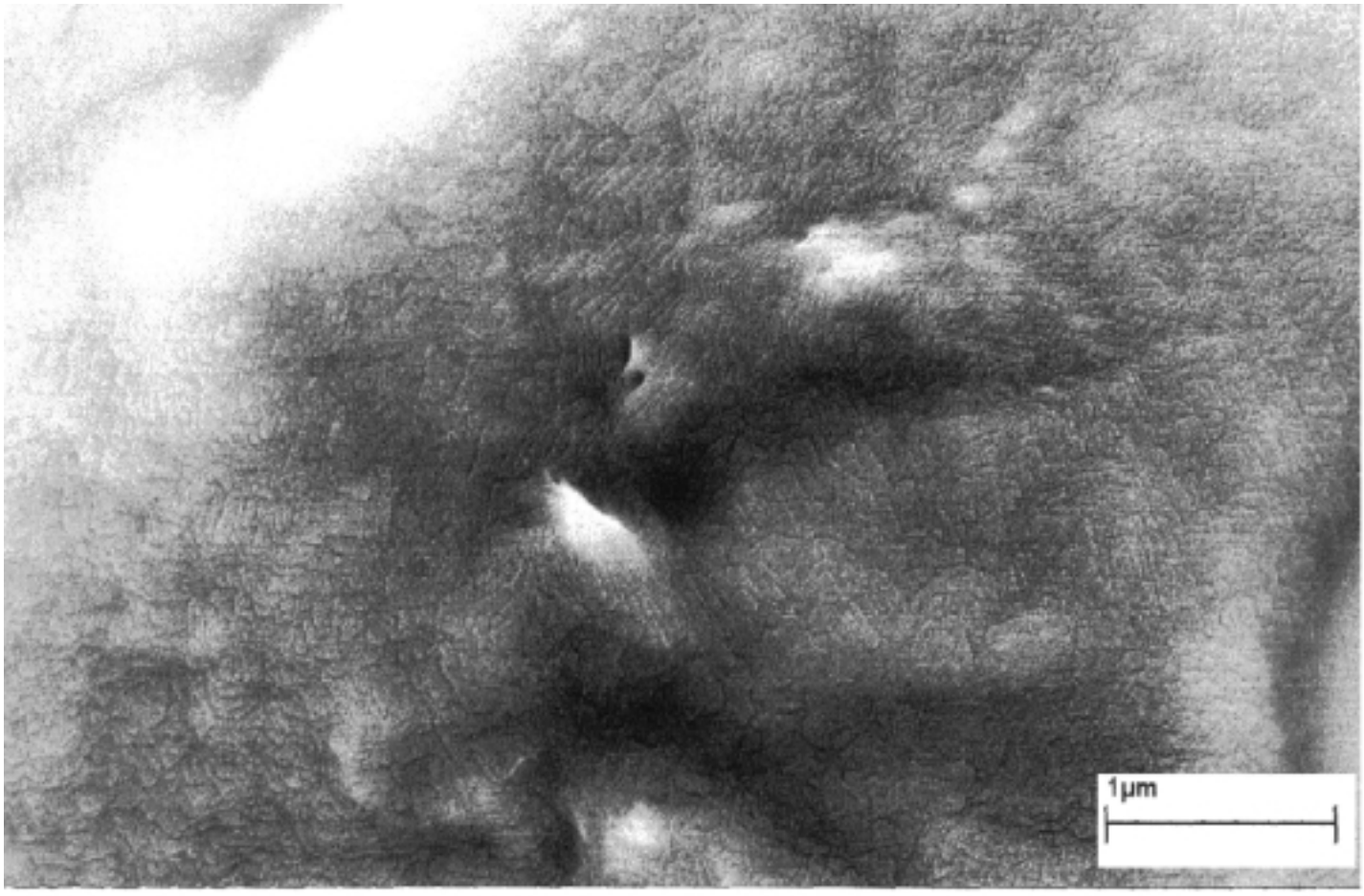

Figure 29. SEM Micrograph of Polycarbonate Lamellae Growing Parallel to the Substrate After 7 Days of Crystallization at 190°C

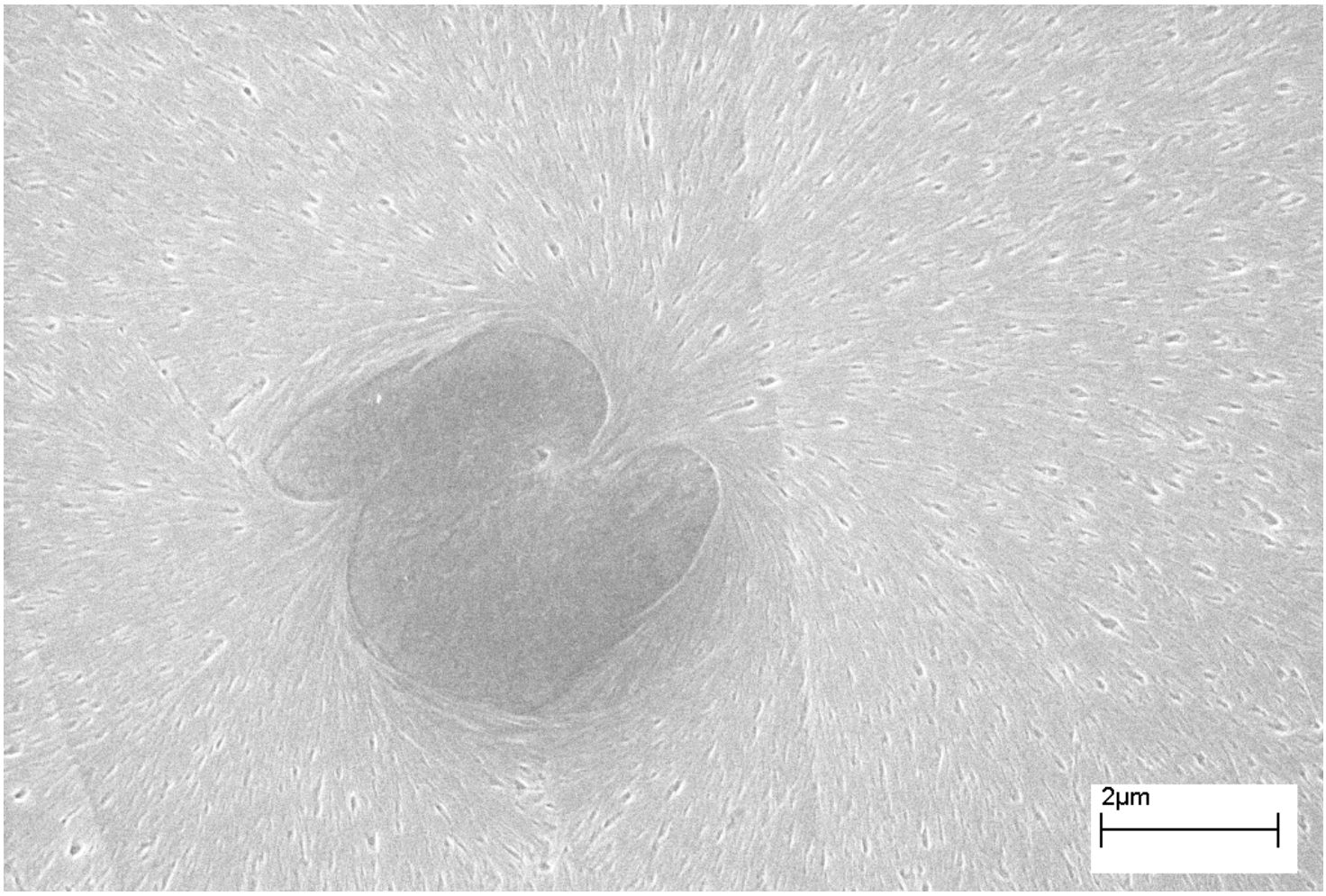

Figure 30. Spherulitic Structure of Polycarbonate Crystallized on Calcite at 190°C

found, making it difficult to prepare samples for measurements. Because of the inconsistencies of epitaxial growth of polycarbonate on calcite, the study of lamellar thickening by annealing at higher temperatures was not carried out using thin films of polycarbonate.

5.2 Discussion

Differential scanning calorimetry was performed to observe the shift of the melting point of polycarbonate with annealing time. Samples for both annealing temperatures were to be crystallized at 190°C, but because of instrumental problems with the oven, the samples were crystallized at different temperatures. In looking at the heating traces of the unannealed sample for both sets of samples, the actual crystallization temperature can be determined by using the Hoffman-Weeks equation (Equation 16).

$$T_f^* - T_f = \phi \ (T_f^* - T_c) \tag{16}$$

Knowing the lower endotherm melting point, the crystallization temperature can be calculated. The difference in crystallization temperature makes the direct comparison of data somewhat ambiguous, but the relationship between the melting point and lamellar thickness, as defined in the Gibbs-Thomson equation, is independent of crystallization temperature.

Samples annealed at 223°C show a shoulder in the heating traces until the annealing time has increased to above 60 minutes. The melting point of polycarbonate after annealing at 223°C shifts approximately 5°C when annealed for 600 minutes. The range of shift is much less than that observed by Sohn in his study of 28,000 molecular weight polycarbonate.[17] The higher annealing temperature was used for the second set of

samples in an attempt to increase the shift in melting temperature. A variation in crystallization temperature should not affect the extent to which the melting point shifts to higher temperature, but increasing the annealing temperature should increase the difference in melting temperature because the lamellae are given more thermal energy to rearrange. After preparing and running the samples annealed at 228°C, there was not a larger increase in melting point shift. This may be attributed to the molar mass of the polymer, as it is lower than the polycarbonate used by Sohn. The heating traces for samples annealed at 228°C have no variation in shape because the annealing temperature, determined using results from the 223°C samples, is near the actual melting temperature of the polycarbonate samples.

Because there is not a large variation in the melting temperature of the polycarbonate samples, the variation in lamellar thickness will not be large. Peaks in the plots of intensity vs. scattering vector for the samples annealed at both 223° and 228°C shift very little with annealing time. The samples annealed at 223°C show a range of long spacings from approximately 130Å to 180Å, giving lamellar thicknesses from 35Å to 54Å. The first three annealing times (0, 30, and 60 minutes) show no variation in lamellar thickness, but beyond 60 minutes of annealing, the thickness begins to shift with annealing time. It is expected that the maximum lamellar thickness should occur after the longest annealing time, and this trend is held up when experimental error is taken into account. The lamellar thickness data were assumed to have an error of ± 5Å considering the sensitivity of the small-angle X-ray technique. The results for samples annealed at 228°C give less insight into the relationship between annealing time and lamellar thickness because the thicknesses calculated are essentially constant within experimental

error. The lack of shift in melting point and lamellar thickness is probably due to the over heating of the polymer crystals upon annealing. The data collected from small-angle X-ray scattering give very little information when analyzed individually, but the comparison of the data from the two annealing temperatures with data in literature yields more definitive conclusions for the equilibrium melting temperature and surface free energy of the crystal.

The Gibbs-Thomson plot, shown in Figure 24, shows the linear relationship between melting temperature and the inverse of lamellar thickness. After compiling the data, the results from this study and the studies of Jonza et al. and Sohn can be described with a linear fit. The value of the equilibrium melting temperature from this fit is 303°C, and the surface energy, calculated from the slope, is 36.6mJ/m^2. The equilibrium melting point is approximately 20°C less than the values determined by Jonza et al. and Sohn.[16,17] This difference in equilibrium melting temperature may be associated with the large uncertainty of the lamellar thickness determination, combined with the rather small range over which the thickness varies and the length of the extrapolation to obtain the equilibrium melting temperature. Another reason for the difference between the equilibrium melting temperature calculated in this work and reported in the literature is difference in molar mass of the polycarbonate sample used in the various studies. BAPC in the present study is characterized by a weight average molar mass of 19,000 g/mol, which is considerably less than that of samples used in the other studies, (37,000g/mol and 28000g/mol, respectively). It is well known and proved by thermodynamic means that the equilibrium melting temperature increases with molar mass and levels off only for molar masses in the range of 100,000 g./mol. The variation in equilibrium melting

temperature with chain length is especially important in the low molar mass range. A more systematic study using significantly different annealing temperatures and annealing treatments should be performed to determine a more reliable value of the equilibrium melting temperature and surface energy.

One aspect of this project was to determine if microscopy is a viable technique to measure lamellar thickness in semi-crystalline polymers. The use of atomic force microscopy requires the morphology of the polymer to be present and visible on the surface of the sample. Hot pressed films show no surface morphology, so the sample has to be microtomed or fractured to see into the bulk. Microtoming is known to sometimes lead to artifacts in images of the morphology of semi-crystalline polymers because the cutting unless carried out at very low temperatures leads to plastic deformation of the material. The same issues hold true for polycarbonate samples, as displayed in the micrographs in the results section. The use of an etchant on a fractured surface is a promising way to expose the bulk morphology, but the concentration of etchant and exposure time need to be optimized in order to accurately measure the thickness of lamellae.

The epitaxy of polycarbonate on a substrate would enable (1) the study of the lamellae thickness by microscopic techniques and (2) the comparison between thin film and bulk morphologies in terms of the Gibbs-Thomson equation. The accuracy of long spacing measurements in the solution cast samples on calcite substrates is unknown because the lamellae are assumed to be edge-on. The long spacing determined for the thin film, 151Å, is slightly larger than that of the unannealed bulk sample shown in Figure 18, 132Å. This difference in long spacing cannot be solely attributed to

uncertainties in measurements and may be a further indication that surface morphology differs from bulk morphology.[20] One should also keep in mind that the long spacing measured by atomic force microscopy is a number average value, while that obtained from SAXS using the Bragg law is closer to a weight average. Even if the long spacing in the polycarbonate thin films is known, the comparison using the Gibbs-Thomson relationship requires the calculation of lamellar thickness and determination of melting point, both of which are difficult for thin films on a substrate such as calcite. Organic substrates, such as p-terphenyl, would allow for easier measurements of melting point, but samples could not be prepared for isothermal crystallization of the polycarbonate.

5.3 Conclusions

This study of polycarbonate crystallization has encountered many obstacles, only few of which could be overcome. Within the experimental uncertainty associated with the estimation of lamellar thicknesses and with the effect of molar mass, the calorimetry and small-angle X-ray scattering data obtained in this study and from the literature show a linear relationship between the melting temperature and the inverse of the lamellar thickness. The linear behavior of the data gives information about thermodynamic constants of polycarbonate, (1) the equilibrium melting temperature and (2) the free energy of the fold surface of the lamellae. Until this study, the equilibrium melting temperature and surface free energy of polycarbonate had only been measured by two researchers using three data points each. Results from these experiments have added numerous data points to the Gibbs-Thomson plot to give values of the material constants that are lower than previously reported. In this study, the equilibrium melting temperature was found to be 303°C, which is over 20°C lower than the previously

reported values. The surface free energy of polycarbonate was calculated to be 36.6mJ/m^2, whereas previous work reports values of 52 and 70mJ/m^2. More experiments must be performed on polycarbonate, using various annealing temperatures and annealing times to gain a more accurate value of the equilibrium melting temperature and surface free energy.

The second part of this study was to compare the bulk polycarbonate lamellar thickness with the lamellar thickness of polycarbonate thin films. Because of surface constraints of the polymer, the thin film morphology may be different from that of the bulk material. Making thin films of polycarbonate for lamellar thickness measurements proved to be a difficult task. To get an accurate measurement of the lamellar thickness, the lamellae need to form edge-on. Polycarbonate does not, however, consistently grow epitaxially on the substrates used during this study (calcite, silicon, and p-terphenyl). A few samples did show partial epitaxy, and from those samples a long space was measured, which is comparable to the long spacings measured by small-angle X-ray scattering.

Chapter 6. Future Work

Various conclusions as to the crystallization behavior of polycarbonate have been given for both the initial stages of crystallization and the secondary stage of crystallization. Even with the conclusions drawn and described in individual chapters, research on the crystallization of polycarbonate and other polymers is not exhausted. This chapter gives a few ideas and suggestions for work that would add to the conclusions given here.

6.1 Initial Stages of Crystallization

Although polymers have been reported to show an ordering process prior to the nucleation and growth of primary crystals, there is not necessarily one universal behavior for all polymers during the induction period. Akpalu and Amis demonstrated that ordering prior to crystallization might be a consequence of a large molecular weight distribution. Results of this study of the initial stages of crystallization for a polydisperse bisphenol A polycarbonate sample may suggest a different interpretation. Differences in the time scale characteristic for the induction period were obtained by wide angle X-ray diffraction and differential scanning calorimetry. This difference can be interpreted in terms of sensitivity between these two techniques. Similarly, it is very likely that small angle scattering is more sensitive that wide angle X-ray diffraction. A supporting argument for this proposal is found in the apparent correlation between induction time and crystallization half time.

Because the sensitivity of each experimental technique is important in the conclusions drawn from studies on the initial stages of crystallization, it would be

beneficial to investigate whether the nucleation density of the polymer sample is large enough to ensure that the early stages of crystallization are observed by the time 1% crystallinity is detected. Using the optical microscope, the number of nuclei in a given volume can be estimated from the number of spherulites per unit volume, as each nucleus gives rise to a spherulite, and assuming an average nucleus size, the volume of the nucleus could be determined. The volume of the nucleus multiplied by the number of nuclei will give the total volume of nuclei in the polymer sample observed in the microscope. The ratio of the volume of nuclei to the sample volume will give a volume fraction of nuclei. If the volume fraction of nuclei is larger than the sensitivity of a given experimental technique, then results collected will be based on nucleation as opposed to the induction period, prior to nucleation and growth.

More accurate experiments should be carried out with narrow molar mass distribution samples to investigate whether the induction times determined at a given temperature for different fractions correlate for a given polymer with the crystallization half times. Such a study would definitely provide a better understanding of the peculiar results reported for PEKK, PET and it-PP may explain these simply in terms of sensitivity arguments.

The use of neutron scattering could be helpful in determining if liquid-liquid phase separation on the basis of molar mass is at the origin of the observed small angle X-ray scattering evolution during the induction period. The lower molar mass polycarbonate chains could be labeled with deuterium and small-angle neutron scattering could detect the phase separation, or lack thereof, of these shorter chains from the longer chains in the polymer sample. One problem with such an experimental approach is that

phase separation could also be driven by deuteration. However, if the magnitude of the scattering vector characterizing the length scale of the fluctuations in the SAXS experiment is comparable to that determined by neutron scattering, then one could argue that phase separation of lower molar mass (less flexible) polymer chains from higher molar mass (more flexible) chains is at the origin of the peculiar density and orientation fluctuations observed by scattering methods during the induction period.

Other polymer systems should also be studied so that one can fully understand why the onset of small angle scattering is observed in PEEK, it-PP and PET during the induction period (as determined by DSC) and not observed in other polymers such as PE and bisphenol A polycarbonate.

6.2 Isothermal Lamellar Thickening

There is a great deal of work that can be done to add to the results pertaining to the isothermal lamellar thickening of polycarbonate. Because there is such a large difference between the values of equilibrium melting temperature and surface free energy calculated here and the values reported in literature, the study of more annealing temperatures and times will help refine the accuracy with which we can estimate these material constants. The results that are presented here show that the effect of crystallization temperature on the studies of lamellar thickening are negligible, but a more systematic study may be in order.

The epitaxial growth of polycarbonate on various substrates (i.e. calcite and p-terphenyl) is promising because epitaxy has been achieved on both substrates. With calcite as a substrate in this study, the long spacing of some polycarbonate samples could be measured using scanning electron microscopy, but there were many samples observed

that did not demonstrate epitaxial growth. Optimizing the preparation technique that gives edge-on lamellae on a calcite substrate would allow more samples to be prepared and enable further studies of lamellar thickening as a function of annealing time. Identifying other substrates on which polycarbonate may grow epitaxially is another possibility for continuing work on the lamellar thickness of thin film polycarbonate. P-terphenyl is a prime candidate as a substrate if the sublimation process can be limited as the polycarbonate isothermally crystallizes. Large crystals (mm scale) of p-terphenyl could be formed using the sublimation process, and these crystals could be used with hot pressed thin films of polycarbonate to force epitaxial lamellar formation in the film.

Preliminary experiments were performed on bulk polycarbonate samples to see if the lamellar thickness could be measured using microscopy techniques. Samples etched in diethyletriamine and triethylamine showed promising results for measuring the lamellar thickness in the bulk directly from the micrographs. Once proper conditions for etching (etchant concentration and time in the etchant) are determined, the bulk lamellar thickness can be measured directly using microscopy.

Because lamellar thickness could not be determined using microscopy, small-angle X-ray scattering is the best technique in determining the lamellar thickness of polymer samples. The various methods allowing estimation of the lamellar thickness from small-angle X-ray scattering curves needs to be examined further. Use of the Bragg law on Lorenz corrected scattering curves assumes that the bulk crystallinity is the same as the local crystallinity. If this assumption does not hold true, other methods of analysis, such as the correlation or the interface distribution function approaches, need to be employed. Further investigations will require recording the scattering data over larger

scattering angular range so that the proper extrapolation of scattering intensity to very high q can be carried out and the correlation and interface distribution functions calculated. This will enable the determination of lamellar thickness by different methods and compare these results with those obtained by the Bragg law. This would further provide a way to compare local and bulk crystallinities.

References

1. Bassett, D. C. Principles of Polymer Morphology. Cambridge: Cambridge University Press, 1981.
2. Shultz, J. Polymer Material Science. New Jersey: Prentice Hall Inc., 1974
3. Hannay, N. B., ed. Treatise on Solid State Chemistry: Volume 3 Crystalline and Noncrystalline Solids. New York: Plenum Press, 1976
4. Hsiao, B.; Gardner, K.; Wu, D.; Chu, B. *Polymer* **1993**, *34*, 3986-3996
5. Weeks, J. *Journal of Research of the National Bureau of Standards – A. Physics and Chemistry* **1963**, *67A*, 441-451
6. Alizadeh, A.; Sohn, S.; Quinn, J.; Marand, H.; Shank, L.; Iler, H. *Macromolecules* **2001**, *34*, 4066-4078
7. Marand, H.; Alizadeh, A.; Farmer, R.; Desai, R.; Velikov, V. *Macromolecules* **2000**, *33*, 3392-3403
8. Imai, M.; Mori, K.; Mizukami, T.; Kaji, K.; Kanaya, T. *Polymer* **1996**, *33*, 4451-4456
9. Imai, M.; Kaji, K.; Kanaya, T. *Phys. Rev. Let.* **1993**, *71*, 4162-4165
10. Imai, M.; Kaji, K.; Kanaya, T.; Sakai, Y. *Phys. Rev. B.* **1995**, *52*, 12696-12704
11. Terrill, N.; Fairclough, P.; Towns-Andrews, E.; Komanschek, B.; Young, R.; Ryan, A. *Polymer* **1998**, *39*, 2381-2385
12. Ezquerra, T.; Lopez-Cabarcos, E.; Hsiao, B.; Balta-Calleja, F. *Phys. Rev. E.* **1996**, *54*, 989-992
13. Akpalu, Y.; Amis, E. *J. Chem. Phys* **1999**, *111*, 8686-8695
14. Akpalu, Y.; Amis, E. *J. Chem. Phys* **2000**, *113*, 392-403
15. Mezghani, K.; Campbell, R.; Phillips, P. *Macromolecules* **1994**, *27*, 997-1002
16. Jonza, J.; Porter, R. *J. Poly. Sci., Polym. Phys.* **1986**, *24*, 2459-2472
17. Sohn, S. Crystallization Behavior of Bisphenol A Polycarbonate: Effects of Crystallization Time, Temperature, and Molar Mass. Ph.D. Dissertation, Virginia Polytechnic Institute & State University, Blacksburg, VA, 2000.
18. Verma, R.; Velikov, V.; Kander, R.; Marand, H. *Polymer* **1996**, *37*, 5357-5365
19. Wang Z-G.; Hsiao, B.; Fu, B.; Liu, L.; Yeh, F.; Sauer, B.; Chang, H.; Schultz, J. *Polymer* **2000**, *41*, 1791-1797
20. Zhou, H.; Wilkes, G. *Polymer* **1997**, *28*, 5735-5747
21. Qian, X.; Rickert, S.; Lando, J. *J. Mater Res* **1989**, *4*, 996-1004
22. Wittmann, J-C.; Lotz, B. *Prog. Polym. Sci.* **1990**, *15*, 909-948
23. Lotz, B., Private Communication
24. Chu, B.; Harney, P.; Li, Y.; Linliu, K.; Yeh, F.; Hsiao, B. *Rev. Sci. Instrum.* **1994**, *65*, 597-602

Vita

Robin Farmer was born April 15th, 1978 in Pullman, Washington. She grew up both in Washington and in Charlottesville, Virginia. She entered Virginia Polytechnic Institute and State University to obtain an undergraduate degree in Materials Science and Engineering. She decided to pursue a Master's degree in Materials Science and Engineering and joined a five-year Bachelor/Master program. After completion of her Master's degree, Robin will work for her Doctorate at the University of Delaware in Materials Science and Engineering with a focus on biopolymers.